Supplementary Information (SI)

Rapid and Accurate Visualization of Breast Tumors with a Fluorescent Probe Targeting α-Mannosidase 2C1

Kyohhei Fujita[1], Mako Kamiya[1,3], Takafusa Yoshioka[1], Akira Ogasawara[2], Rumi Hino[4], Ryosuke Kojima[1,3], Hiroaki Ueo[5] and Yasuteru Urano[*1,2,6]

[1]Graduate School of Medicine and [2]Graduate School of Pharmaceutical Sciences, The University of Tokyo, 7-3-1 Hongo, Bunkyo-ku, Tokyo 113-0033, Japan. [3]PRESTO, Japan Science and Technology Agency, 4-1-8 Honcho, Kawaguchi, Saitama 332-0012, Japan. [4]Daito Bunka University, Department of Sports and Health Science, 560 Iwadono, Higashimathuyama, Saitama, 355-8501, Japan. [5]Ueo Breast Cancer Hospital, Oita, 870-0854, Japan. [6]CREST, Japan Agency for Medical Research and Development, 1-7-1 Otemachi, Chiyoda-ku, Tokyo 100-0004, Japan.

*e-mail uranokun@m.u-tokyo.ac.jp

Table of Contents

Optical properties of probes. Ultraviolet-visible spectra were obtained on a V-2450 spectrometer (Shimadzu Corporation) and fluorescence spectra were obtained on a F-7000 fluorescence spectrometer (Hitachi High-Technologies Corporation). Probes were dissolved in dimethyl sulfoxide (DMSO) to obtain stock solutions. Optical properties of probes were examined in PBS containing 0.1% DMSO *v*/*v* as a co-solvent (**Figures S6** and **S17**).

Measurement of α-mannosidase activity *in vitro*. The time course of fluorescence intensity of HMRef-αMan was monitored at excitation/emission wavelengths of 498 nm/540 nm on a F-7000 fluorescence spectrometer (Hitachi High-Technologies Corporation). To a 10 μM solution of HMRef-αMan in 3 mL of PBS (-), pH 7.4, containing 0.1% DMSO as a cosolvent, α-mannosidase (SIGMA M7257, 2.4 units) was added at 150 s. The gray line (control) shows the fluorescence change in the absence of α-mannosidase (**Figure S6**).

Measurement of GGT activity *in vitro*. The time course of fluorescence intensity of gGlu-2OMe SiR600 was monitored at excitation/emission wavelengths of 595 nm/615 nm on a F-7000 fluorescence spectrometer (Hitachi High-Technologies Corporation). To a 10 μM solution of gGlu-2OMe SiR600 in 3 mL of PBS (-), pH 7.4, containing 0.1% DMSO as a cosolvent, GGT (Oriental Yeast Co., Ltd., 50 units) was added at 150 s. The gray line (control) shows the fluorescence change in the absence of GGT (**Figure S18**).

***Ex-vivo* fluorescence imaging of fresh surgical FA, PT and ICP specimens from human breast**. A 50 μM solution of HMRef-αMan (3-10 mL) in PBS containing 0.5% *v*/*v* DMSO as a co-solvent was added to a 3.5 or 5.0 cm dish containing a human surgical specimen so that the tissue was completely soaked with probe solution. The fluorescence images were recorded using an in-house-built portable fluorescence imager. Surgical specimens were evaluated 10 min after resection. The results are summarized in **Figures S11** and **S12**.

Immunohistochemical analysis of PTEN expression. Formalin-fixed paraffin-embedded tissues were sectioned at 4 μm thickness. Immunoperoxidase staining for PTEN (mouse monoclonal antibody, Clone: PTN-18, Lot: 061K4889, Sigma-Aldrich, Inc., Saint Louis, Missouri 63103, U.S.A.) was performed using a Ventana Benchmark XT (Ventana Medical Systems) automated slide staining system. Sections were deparaffinized, pretreated with Cell Conditioning 1 (CC1, Ventana Medicals Systems), reacted with primary antibodies for 32 min at room temperature, visualized with a Ventana DAB detection kits; (iView DAB detection kit) and counter-stained with Hematoxylin and Bluing Reagent. PTEN antibody was diluted to 1/25, and used with the iVIEW DAB detection kit and Endogenous Biotin blocking kit (Ventana Medical Systems). Human breast tissues were used a positive control of PTEN immunostaining. Negative controls were conducted by adding REAL Antibody Diluent (Dako), instead of the primary antibody. The results are summarized in **Figure S23**.

Immunohistochemical analysis of phospho-AKT (pSer473) expression. Formalin-fixed paraffin-embedded tissues were sectioned at 4 μm thickness. Immunoperoxidase staining for phospho-AKT (pSer473) (rabbit polyclonal antibody, Clone: PSER473, Lot: 129187004, Sigma-Aldrich, Inc., Saint Louis, Missouri 63103, U.S.A.) was performed using a Ventana Benchmark XT (Ventana Medical Systems) automated slide staining system. Sections were deparaffinized, pretreated with protease-1 (Protease1, Ventana Medicals Systems), reacted with primary antibodies for 32 min at room temperature, visualized with a Ventana DAB detection kit (iView DAB detection kit) and counter-stained with Hematoxylin and Bluing Reagent. Phospho-AKT antibody was diluted to 1/50, and used with the iVIEW DAB detection kit and Endogenous Biotin blocking kit (Ventana Medical Systems). Human breast tissues were used as a positive control of phospho-AKT immunostaining. Negative controls were conducted by adding REAL Antibody Diluent (Dako), instead of the primary antibody. The results are summarized in **Figure S23**.

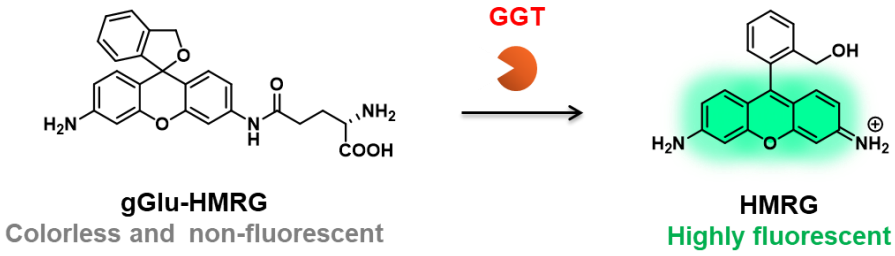

Figure S1. γ-Glutamyltranspeptidase (GGT)-reactive fluorescent probe, gGlu-HMRG.[1]

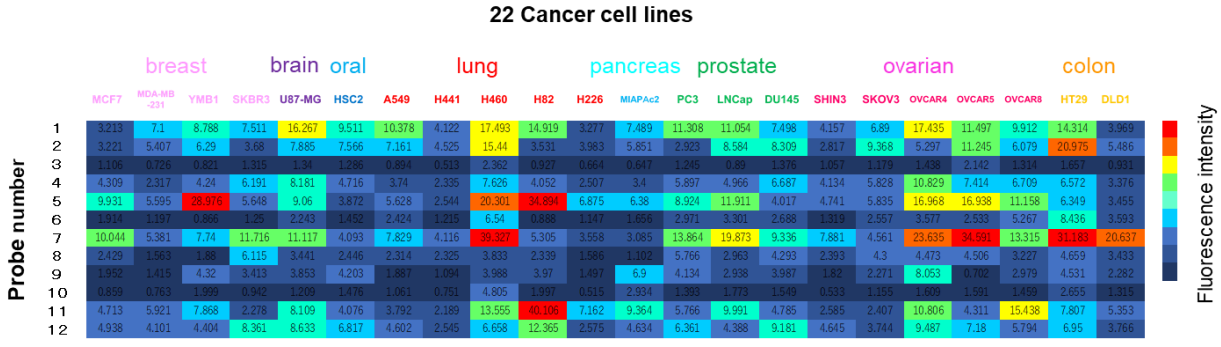

Figure S2. Heat map of intact glycosidase activities in various living cancer cell lines. Fluorescence intensities were quantified by drawing regions of interest (ROIs) on the fluorescence images shown in **Figure 2** (**a**).

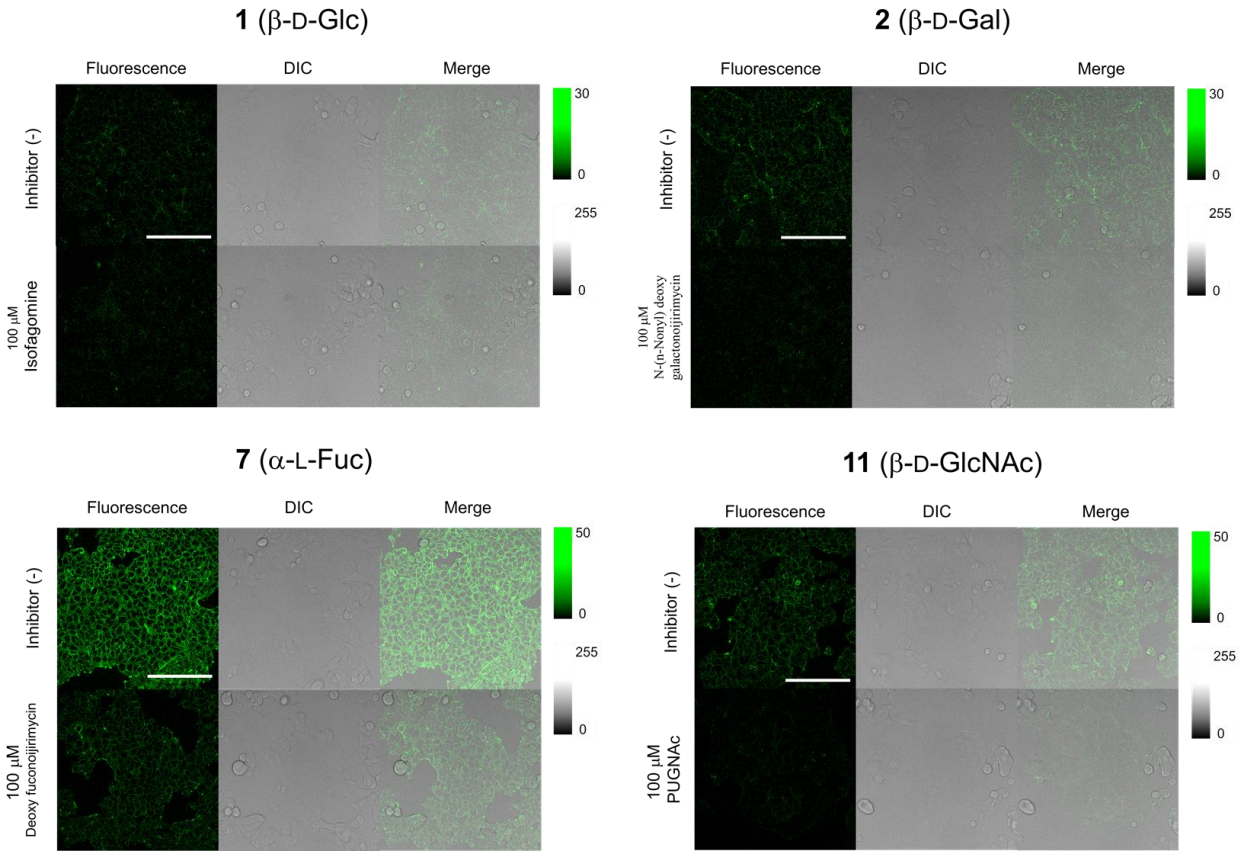

Figure S3. Confocal images of fluorescence intensity in MCF7 cells treated with each glycosidase-reactive probe in the presence and absence of inhibitor. Cells were incubated with 5 μM fluorescent probe in the presence and absence of each inhibitor for 1 h, and fluorescence images were obtained. Ex/Em = 498 nm/505-600 nm. [fluorescent probe] = 5 μM, [inhibitor] = 100 μM. Scale bar, 100 μm.

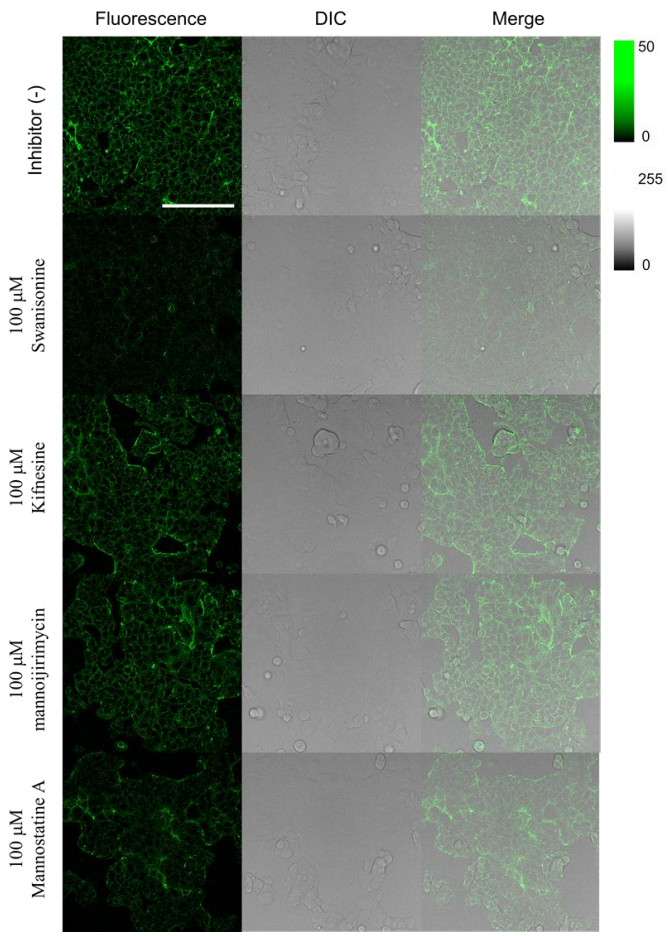

Figure S4. Confocal images of fluorescence intensity in MCF7 cells treated with HMRef-αMan in the presence and absence of 4 inhibitors of α-mannosidase. Cells were incubated with 5 μM fluorescent probe in the presence and absence of each inhibitor for 1 h, and fluorescence images were obtained. Swainsonine significantly inhibited the fluorescence increase of HMRef-αMan in MCF7 cells. Ex/Em = 498 nm/505-600 nm. [HMRef-αMan] = 5 μM, [inhibitor] = 100 μM. Scale bar, 100 μm.

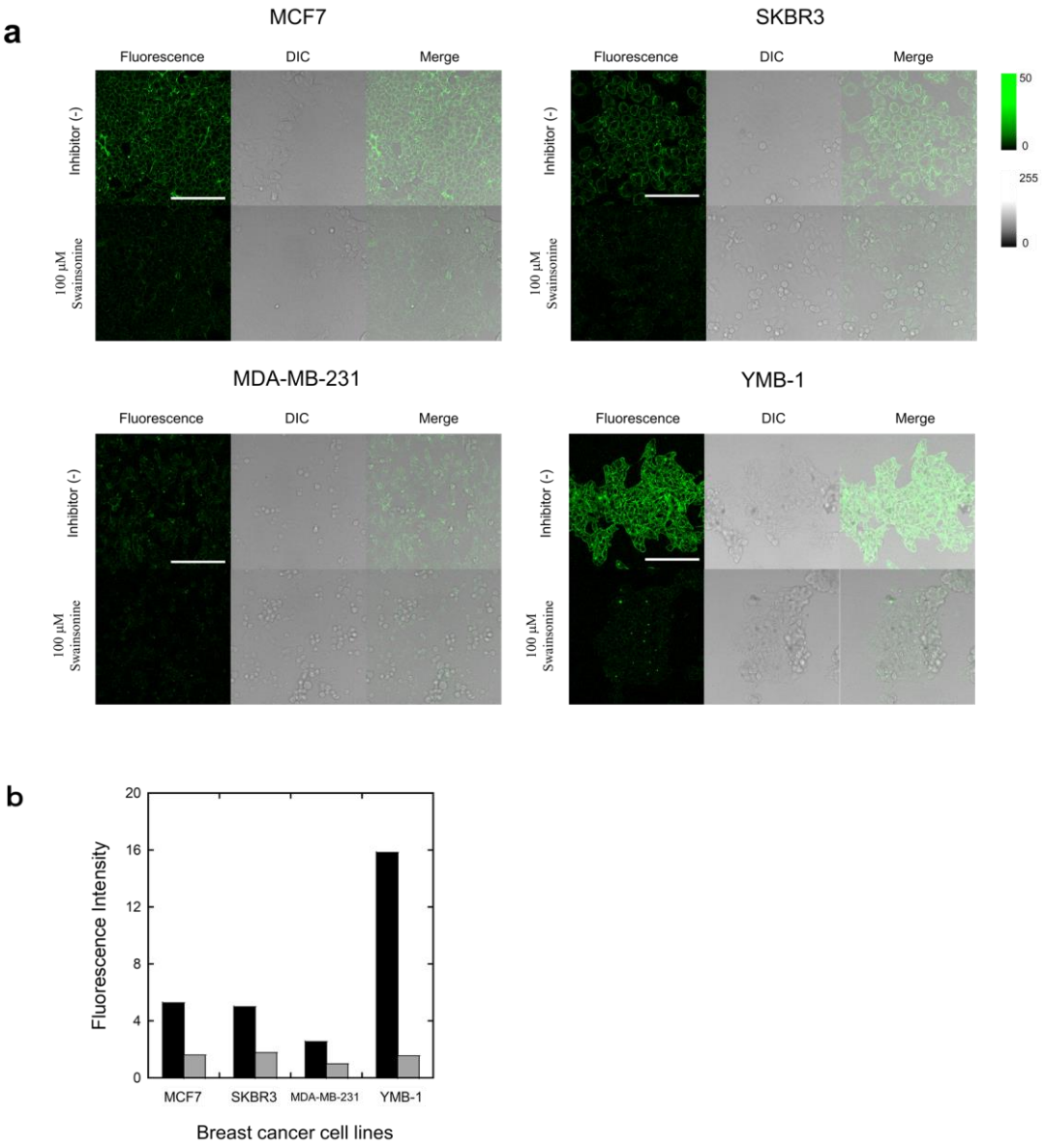

Figure S5. Inhibition of α-mannosidase activity by swainsonine in 4 breast cancer cell lines. (**a**) Confocal images of fluorescence intensity in MCF7, SKBR3, MDA-MB-231 and YMB-1 breast cancer cells treated with HMRef-αMan in the presence and absence of swainsonine. The fluorescence images of MCF7 are the same images shown in **Figure 2** (**d**). (**b**) Fluorescence intensity from each breast cancer cell line. Black bars represent fluorescence intensity in the absence of swainsonine. Gray bars represent fluorescence intensity in the presence of swanisonine. Cells were incubated with 5 μM fluorescent probe in the presence and absence of swainsonine for 1 h, and fluorescence images were obtained. Ex/Em = 498 nm/505-600 nm. [HMRef-αMan] = 5 μM, [swainsonine] = 100 μM. Scale bar, 100 μm.

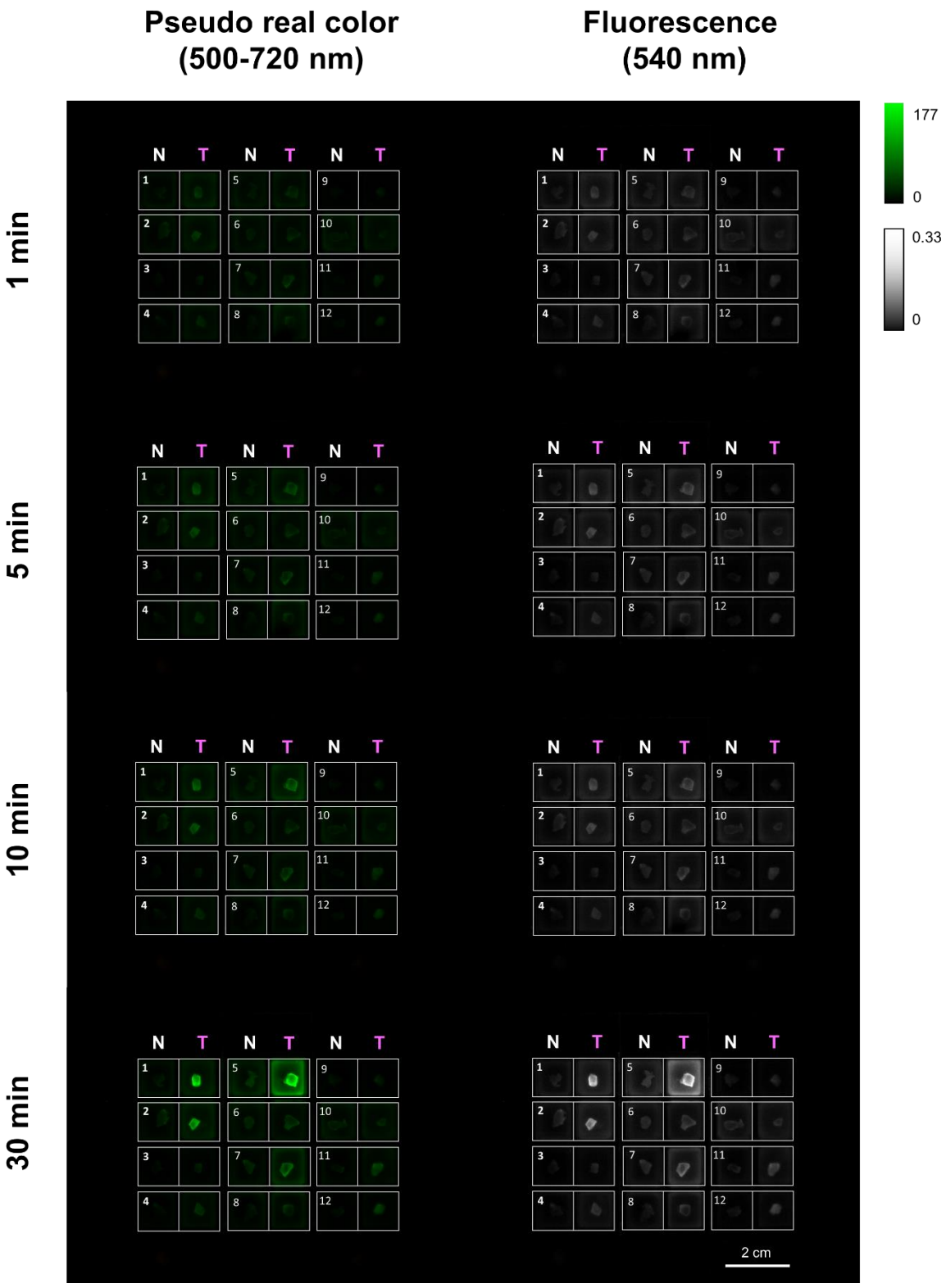

Figure S6. Example of screening using surgically resected normal and IDC tissues from human breast. Exposure time = 100 msec, [fluorescent probe] = 50 μM. Scale bar, 2 cm.

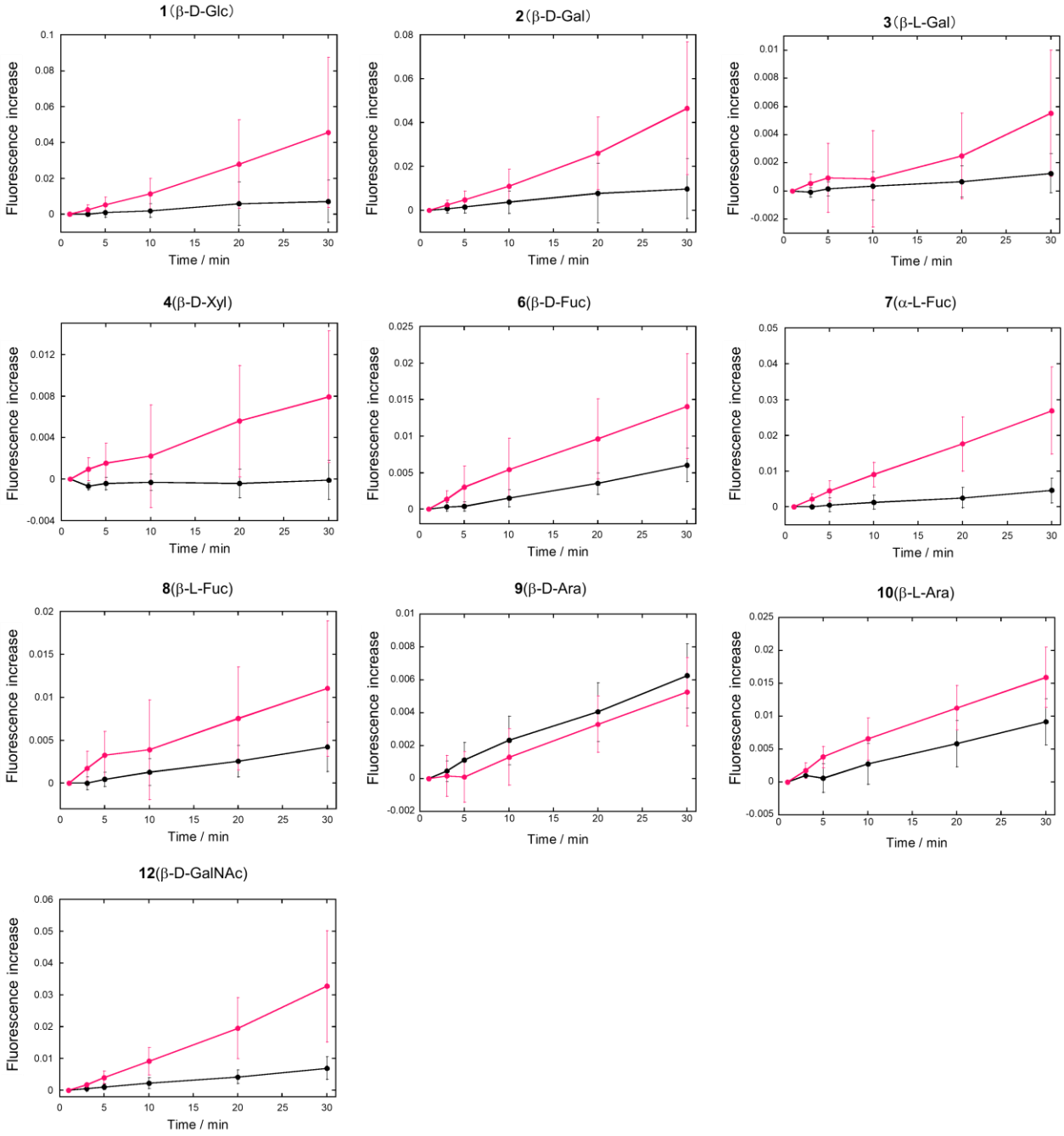

Figure S7. Time-dependent fluorescence increase of each probe in breast cancer tissues. Black lines represent fluorescence increases in normal breast tissues. Pink lines represent fluorescence increases in breast cancer (IDC + DCIS) tissues. Normal (N = 14), IDC (N = 5) and DCIS (N = 3) breast tissues were examined. Error bars represent s.d. [fluorescent probe] = 50 μM.

Table S1. Detection of breast cancer with each fluorescent probe.

HMRef-αMan (Threshold = 0.117)

		diagnosis	
		F.I. positive	F.I. negative
cancer	+	9	1
	-	0	20

Probe **11** (β-D-GlcNAc) (Threshold = 0.083)

		diagnosis	
		F.I. positive	F.I. negative
cancer	+	7	1
	-	2	16

gGlu-HMRG (Threshold = 0.216)

		diagnosis	
		F.I. positive	F.I. negative
cancer	+	8	2
	-	4	15

HMRef-αMan (Threshold = 0.117)
gGlu-HMRG (Threshold = 0.216)

		diagnosis	
		F.I. positive	F.I. negative
cancer	+	10	0
	-	4	15

Breast cancer specimens were diagnosed as F.I. positive (cancer) or F.I. negative (normal) using the indicated threshold values. Calculated PPV, NPV, sensitivity, specificity and AUC are summarized in **Table 1** and **Figure S8**. F.I., Fluorescence increase. AUC, Area under the curve.

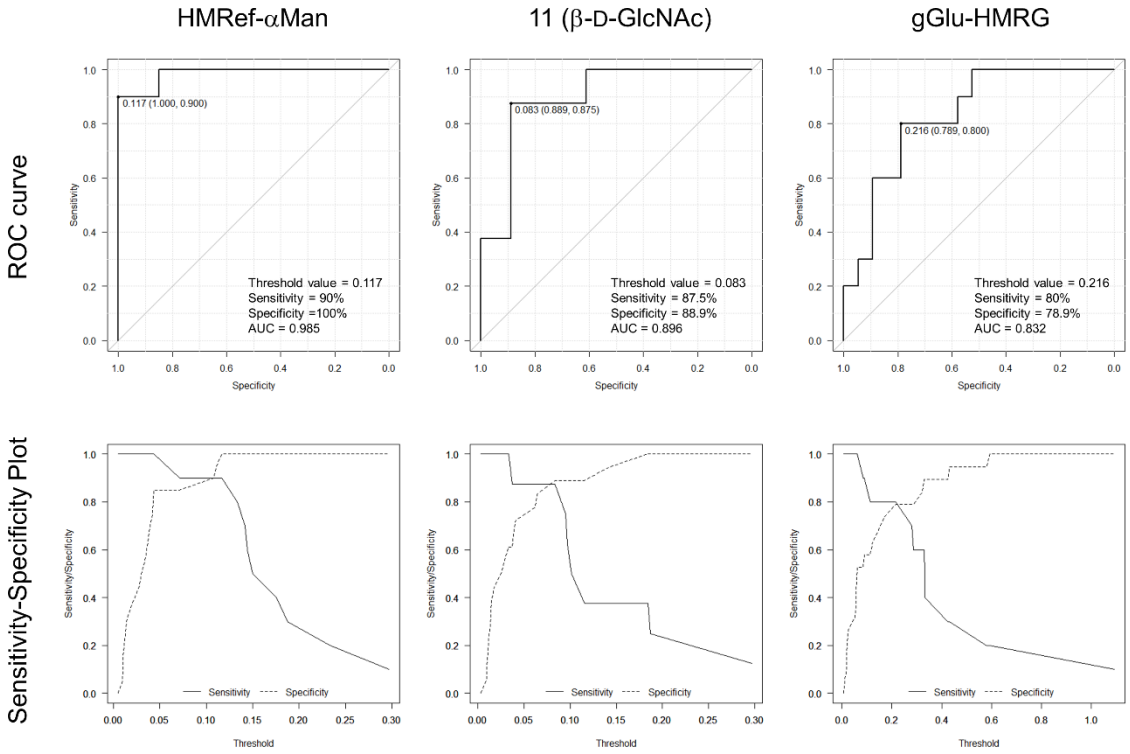

Figure S8. ROC curves and Sensitivity-Specificity plots for breast cancer detection. Threshold value, sensitivity, specificity and AUC of each probe were evaluated from the receiver operating characteristic curve. Normal (N = 20), IDC (N = 7) and DCIS (N = 3) tissues were examined with HMRef-αMan. Normal (N = 18), IDC (N = 5) and DCIS (N = 3) tissues were examined with probe **11** (β-D-GlcNAc). Normal (N = 19), IDC (N = 7) and DCIS (N = 3) tissues were examined with gGlu-HMRG.

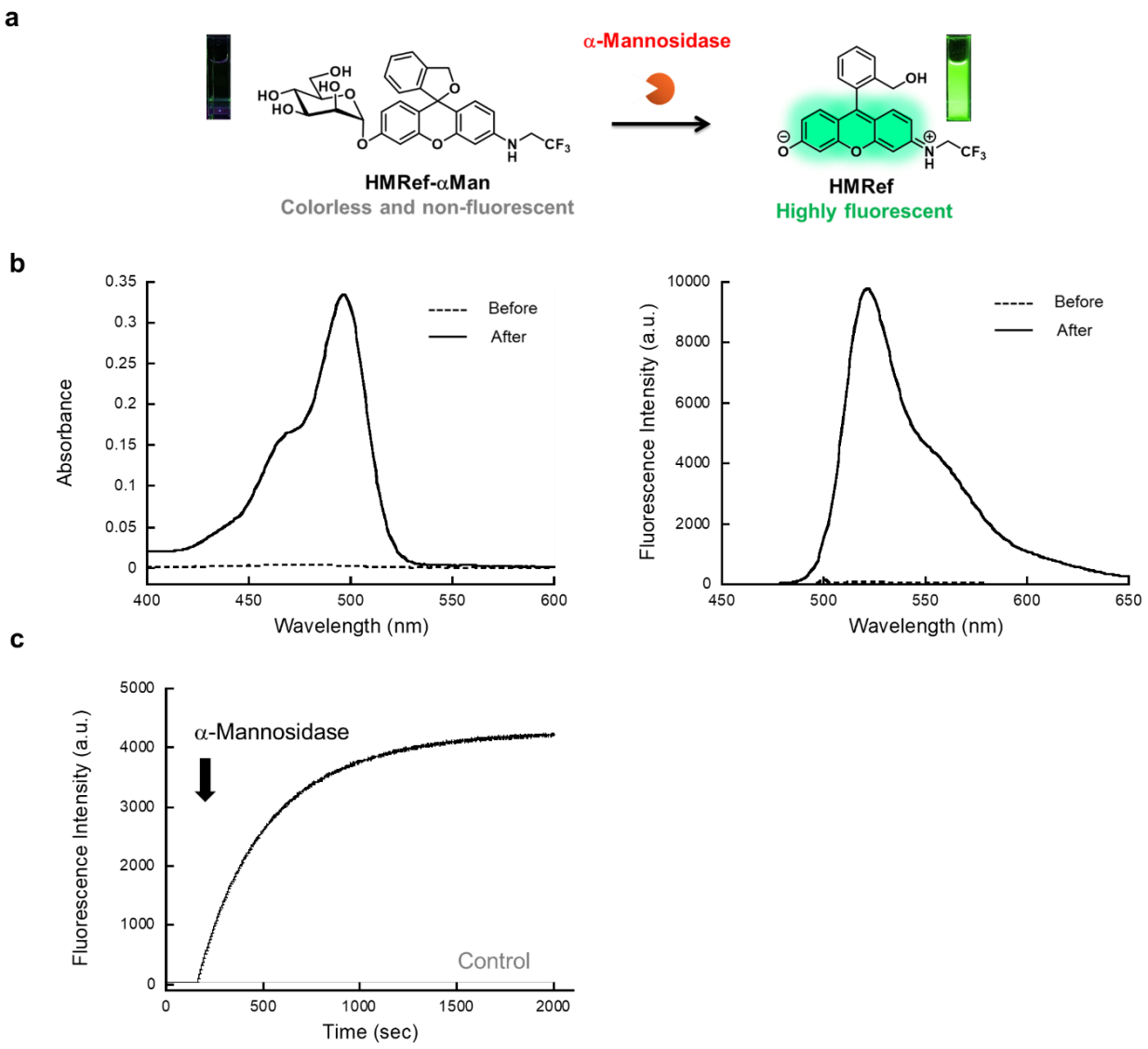

Figure S9. A novel fluorescent probe for α-mannosidase activity. (**a**) Reaction scheme of HMRef-αMan with α-mannosidase. (**b**) Absorption (left) and fluorescence (right) spectra of HMRef-αMan before and after reaction with α-mannosidase. (**c**) The time course of fluorescence intensity of HMRef-αMan upon addition of α-mannosidase from *Canavalia ensiformis* was monitored at excitation/emission wavelengths of 498 nm/540 nm. To a 10 μM solution of HMRef-αMan in 3 mL of PBS (-), pH 7.4, containing 0.1% DMSO as a cosolvent, α-mannosidase (Sigma M7257, 2.4 units) was added at 150 s. The gray line (control) shows the fluorescence change in the absence of α-mannosidase.

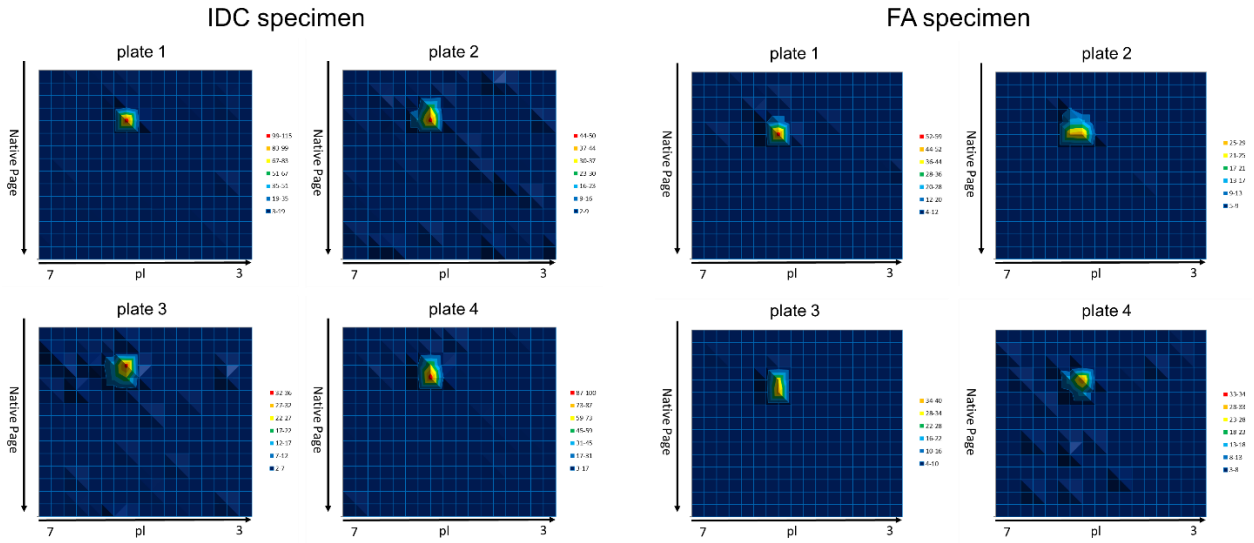

Figure S10. DEG assay using HMRef-αMan with surgically resected IDC and FA specimens from human breast. The assays were carried out as reported.[2] A single fluorescent spot was observed on 2D gels and MAN2C1 was identified by peptide mass fingerprinting analysis. Each lysate sample was evaluated on four gels. Gels were incubated with the probe at 37°C for 12 h. Proteins detected by peptide mass fingerprinting analysis are summarized in **Tables S2** and **S3**. [HMRef-αMan] = 1 μM.

Table S2. List of detected proteins in DEG assay of a human IDC surgical specimen. 115 proteins were identified by peptide mass fingerprinting analysis. MAN2C1 is highlighted in yellow.

	Identified Proteins (115)	Molecular Weight	Protein Identification Probability
1	keratin, type I cytoskeletal 9 [Homo sapiens]	62 kDa	100%
2	complement C3 preproprotein [Homo sapiens]	187 kDa	100%
3	alpha-2-macroglobulin precursor [Homo sapiens]	163 kDa	100%
4	Keratin 10 [Homo sapiens]	59 kDa	100%
5	beta-filamin [Homo sapiens]	278 kDa	100%
6	epidermal cytokeratin 2 [Homo sapiens]	66 kDa	100%
7	filamin-A isoform 2 [Homo sapiens]	281 kDa	100%
8	plectin [Homo sapiens]	532 kDa	100%
9	biglycan preproprotein variant, partial [Homo sapiens]	42 kDa	100%
10	mannosidase, alpha, class 2C, member 1, isoform CRA_a [Homo sapiens]	116 kDa	100%
11	Keratin 5 [Homo sapiens]	62 kDa	100%
12	LMNA protein [Homo sapiens]	53 kDa	100%
13	talin [Homo sapiens]	270 kDa	100%
14	extracellular matrix protein periostin-bm [Homo sapiens]	87 kDa	100%
15	decorin, partial [synthetic construct]	40 kDa	100%
16	Chain A, The Crystal Structure Of Murine P97/vcp At 3.6a	91 kDa	100%
17	collagen type XII alpha-1 [Homo sapiens]	333 kDa	100%
18	Keratin 14 [Homo sapiens]	52 kDa	100%
19	keratin 1 [Homo sapiens]	66 kDa	100%
20	Fibronectin 1 [Homo sapiens]	240 kDa	100%
21	Chain A, Structure Of Human Liver Chichi Alcohol Dehydrogenase (A Glutath ione- Dependent Formaldehyde Dehydrogenase)	40 kDa	100%
22	Chain A, TapasinERP57 HETERODIMER	54 kDa	100%
23	Chain A, Structure Of Human Glutamate Dehydrogenase-Apo Form	56 kDa	100%
24	Fatty acid synthase [Homo sapiens]	273 kDa	100%
25	COL6A3 protein [Homo sapiens]	278 kDa	100%
26	Chain A, Human Serum Albumin In A Complex With Myristic Acid And Tri- Iodobenzoic Acid	66 kDa	100%
27	Homo sapiens adenylyl cyclase-associated protein, partial [synthetic construct]	52 kDa	100%
28	gelsolin isoform b [Homo sapiens]	81 kDa	100%
29	SELENBP1 protein [Homo sapiens]	45 kDa	100%
30	RecName: Full=Glyceraldehyde-3-phosphate dehydrogenase; Short=GAPDH	36 kDa	100%
31	desmoplakin I [Homo sapiens]	332 kDa	100%
32	hornerin precursor [Homo sapiens]	282 kDa	100%
33	Chain A, Crystal Structure Of Wild-type Human Phosphoglucomutase 1	64 kDa	100%
34	WDR1 protein [Homo sapiens]	58 kDa	100%
35	spectrin, alpha, non-erythrocytic 1 (alpha-fodrin), isoform CRA_a [Homo sapiens]	129 kDa	100%
36	Mitochondrial alcohol dehydrogenase isozyme III [Komagataella phaffii GS115]	37 kDa	100%
37	Chain A, Solution structure of the CH domain of human transgelin-2	17 kDa	100%
38	Chain B, Crystal Structure Of S-Nitroso-Nitrosyl Human Hemoglobin A	16 kDa	100%
39	beta-spectrin [Homo sapiens]	275 kDa	100%
40	Chain A, Crystal structure of human vascular adhesion protein-1	85 kDa	100%
41	Chain A, Human Complement Factor B	84 kDa	100%
42	Chain A, Human Muscle L-lactate Dehydrogenase M Chain, Ternary Complex With Nadh And Oxamate	37 kDa	100%
43	PREDICTED: actin, gamma-enteric smooth muscle [Coturnix japonica]	42 kDa	100%
44	TALDO1 protein, partial [Homo sapiens]	37 kDa	100%
45	Chain A, X-Ray Structure Of Human Arginase I: The Mutant D183a In Complex With Abh	35 kDa	100%
46	PREDICTED: junction plakoglobin [Sorex araneus]	80 kDa	100%
47	IGHA1, partial [synthetic construct]	53 kDa	100%
48	filaggrin-2 [Homo sapiens]	248 kDa	100%
49	hypothetical protein EGM_12944, partial [Macaca fascicularis]	281 kDa	100%
50	Chain A, Solution Structure Of Double Super Helix Model	28 kDa	100%
51	leucine aminopeptidase [Homo sapiens]	56 kDa	100%
52	ferritin	20 kDa	100%
53	Chain A, Crystal Structure Of Wild-Type Human Ferritin H Chain	21 kDa	100%
54	keratin, type II cytoskeletal 8 [Macaca mulatta]	54 kDa	100%
55	Chain A, Crystal Structure Of Bovine Serum Albumin	66 kDa	100%
56	hypothetical protein XELAEV_18042575mg [Xenopus laevis]	104 kDa	100%

57	Chain A, Solution structure of the SEA domain of human mucin 1 (MUC1)	8 kDa	100%
58	Chain A, Atomic Cryoem Structure Of Hsp90-cdc37-cdk4 Complex	84 kDa	100%
59	Chain B, Crystal Structure of the Ku Heterodimer	64 kDa	100%
60	Chain A, Crystal Structure Of Sept2 G-Domain	36 kDa	100%
61	desmoglein-1 [Pan paniscus]	114 kDa	100%
62	unnamed protein product [Homo sapiens]	35 kDa	100%
63	Chain E, Leech-Derived Tryptase InhibitorTRYPSIN COMPLEX	23 kDa	96%
64	Complement component 4A (Rodgers blood group) [Homo sapiens]	193 kDa	100%
65	hCG2001591 [Homo sapiens]	193 kDa	100%
66	40-kDa keratin protein, partial [Homo sapiens]	44 kDa	100%
67	Chain A, Annexin A2: Does it induce membrane aggregation by a new m ultimeric state of the protein.	39 kDa	100%
68	Chain B, Crystal structure of alpha5beta1 integrin headpiece (ligand-free form)	51 kDa	100%
69	Cytokeratin-78 [Macaca mulatta]	56 kDa	100%
70	Chain C, Solution Structure Of Human Immunoglobulin M	57 kDa	99%
71	LBA isoform beta [Mus musculus]	310 kDa	99%
72	Chain A, Crystal Structure Of Full-Length Human Peroxiredoxin 4 With T118e Mutation	28 kDa	98%
73	AAA ATPase [Wallemia mellicola CBS 633.66]	90 kDa	97%
74	Chain A, Atpase Domain Of Human Heat Shock 70kda Protein 1	42 kDa	96%
75	Chain A, Crystal Structure Of Recombinant Human Triosephosphate Isomera se At 2.8 Angstroms Resolution. Triosephosphate Isomerase Related Human Genetic Disorders	27 kDa	100%
76	Chain A, Crystal structure of phosphorylated mutant of glyceraldehyde 3-phos phate dehydrogenase from human placenta at 3.15A resolution	36 kDa	100%
77	Chain A, The Refined 1.6 Angstroms Resolution Crystal Structure Of The Co mplex Formed Between Porcine Beta-trypsin And Mcti-a, A Trypsin Inhibitor Of Squash Family	23 kDa	100%
78	Chain O, Glyceraldehyde-3-phosphate dehydrogenase, liver	36 kDa	100%
79	Cyl actin [Tripneustes gratilla]	42 kDa	100%
80	PREDICTED: adenylyl cyclase-associated protein 2 [Pygocentrus nattereri]	52 kDa	100%
81	elongation factor Tu [Mus musculus]	50 kDa	100%
82	keratin, type II cytoskeletal 1 [Pongo abelii]	66 kDa	100%
83	Chain A, Crystal Structure Of Human Peroxiredoxin I In Complex With Sulfiredoxin	22 kDa	100%
84	Chain A, Crystal Structure Of A Single Mutant (n71d) Of Triosephosphate Isomerase From Human	27 kDa	100%
85	Chain B, Model of human IgA2 determined by solution scattering, curve fitting and homology mode	50 kDa	100%
86	immunoglobulin gamma 2 constant region, partial [Homo sapiens]	36 kDa	99%
87	heat shock protein 70 [Trichinella nativa]	71 kDa	98%
88	Elongation factor 1-alpha [Hortaea werneckii EXF-2000]	50 kDa	97%
89	PREDICTED: filamin-A isoform X1 [Rattus norvegicus]	281 kDa	97%
90	put. beta-actin (aa 27-375), partial [Mus musculus]	39 kDa	97%
91	Chain B, Crystal Structure Of The Novel Complex Formed Between Zinc 2- Glycoprotein (Zag) And Prolactin Inducible Protein (Pip) From Human Seminal Plasma	14 kDa	96%
92	BA75_00075T0 [Komagataella pastoris]	47 kDa	95%
93	Chain A, Mhc Class I Molecule B5301 Complexed With Peptide Tpydinqml From Gag Protein Of Hiv2	32 kDa	95%
94	transitional endoplasmic reticulum ATPase [Lobosporangium transversale]	91 kDa	95%
95	unnamed protein product [Dictyostelium discoideum]	43 kDa	94%
96	Protein MAM3 [Malassezia restricta CBS 7877]	77 kDa	93%
97	hypothetical protein BOX15_Mlig026283g2 [Macrostomum lignano]	88 kDa	93%
98	cell division control protein 48 aaa family protein (transitional endoplasmic reticulum at pase),putative [Schistosoma mansoni]	89 kDa	92%
99	PREDICTED: filamin-C-like isoform X1 [Pygocentrus nattereri]	295 kDa	91%
100	Chain A, Bovine Mitochondrial F1-Atpase	55 kDa	90%
101	BA75_02285T0 [Komagataella pastoris]	30 kDa	89%
102	hypothetical protein BN946_scf185000.g91 [Trametes cinnabarina]	47 kDa	88%
103	PIR Superfamily Protein [Plasmodium ovale wallikeri]	40 kDa	87%
104	Chain C, COP9 SIGNALOSOME COMPLEX SUBUNIT 3	48 kDa	86%
105	Chain A, The Structure Of Pentameric Human Serum Amyloid P Component	23 kDa	83%
106	Csa-19 [Homo sapiens]	25 kDa	82%
107	PREDICTED: keratin, type II cytoskeletal 75-like [Monodelphis domestica]	60 kDa	82%
108	LOW QUALITY PROTEIN: 60S ribosomal protein L10a [Loxodonta africana]	23 kDa	79%
109	keratin, type II cytoskeletal 2 epidermal [Meriones unguiculatus]	67 kDa	70%
110	keratin, type I cytoskeletal 13 [Phyllostomus discolor]	49 kDa	45%

111	beta-actin 2 [Sinonovacula constricta]	42 kDa	36%
112	PREDICTED: filamin-B isoform X1 [Jaculus jaculus]	279 kDa	34%
113	immunoglobulin variable region, partial [Homo sapiens]	15 kDa	15%
114	PREDICTED: keratin, type II cytoskeletal 72 [Galeopterus variegatus]	48 kDa	14%
115	hypothetical protein CAPTEDRAFT_205416 [Capitella teleta]	55 kDa	5%

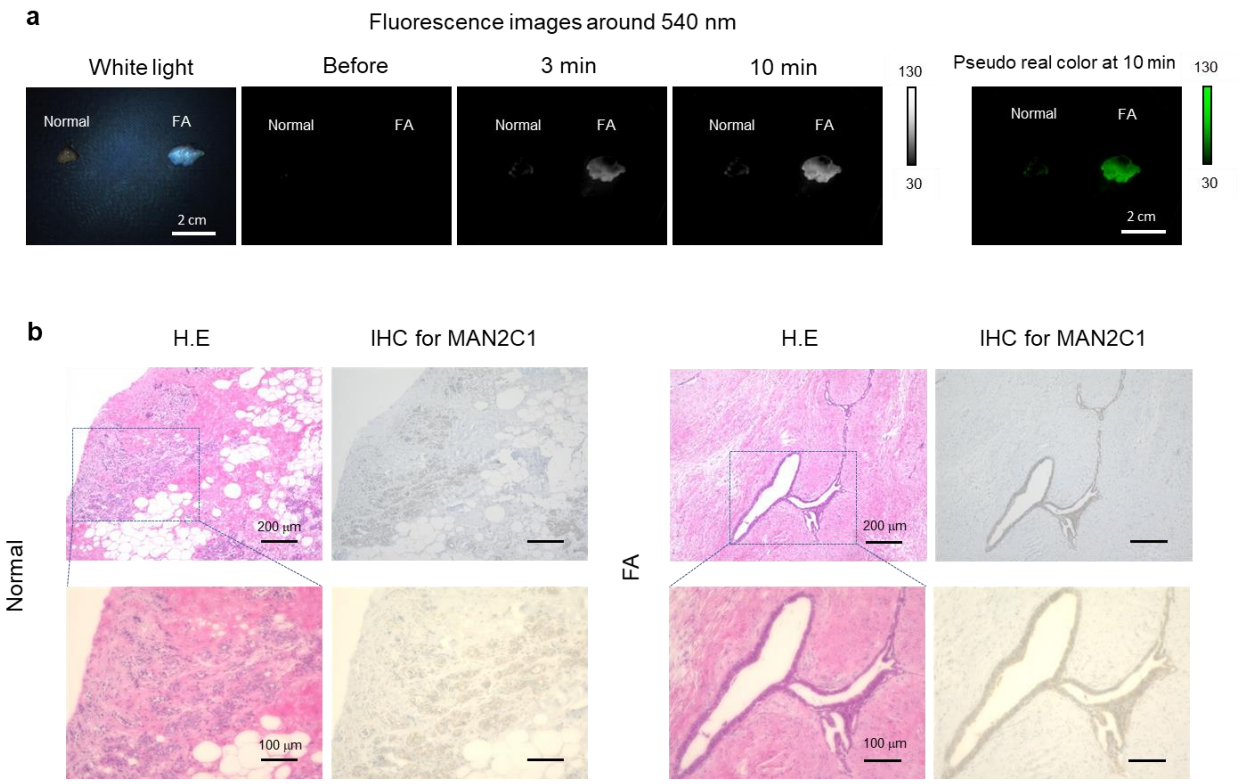

Figure S11. Evaluation of probe HMRef-αMan in surgically resected fresh normal and FA tissues from human breast. (**a**) Time-dependent fluorescence images. The probe showed a significant fluorescence increase only in FA tissue. Surgical specimens were evaluated within 10 min after resection. Probe solution was prepared with PBS (-) containing 0.5 *v*/*v* % DMSO as a co-solvent. [HMRef-αMan] = 50 μM. Scale bar, 2 cm. (**b**) Histological analysis and IHC analysis for MAN2C1 of in the same specimen. Scale bar, 200 μm (upper), or 100 μm (lower).

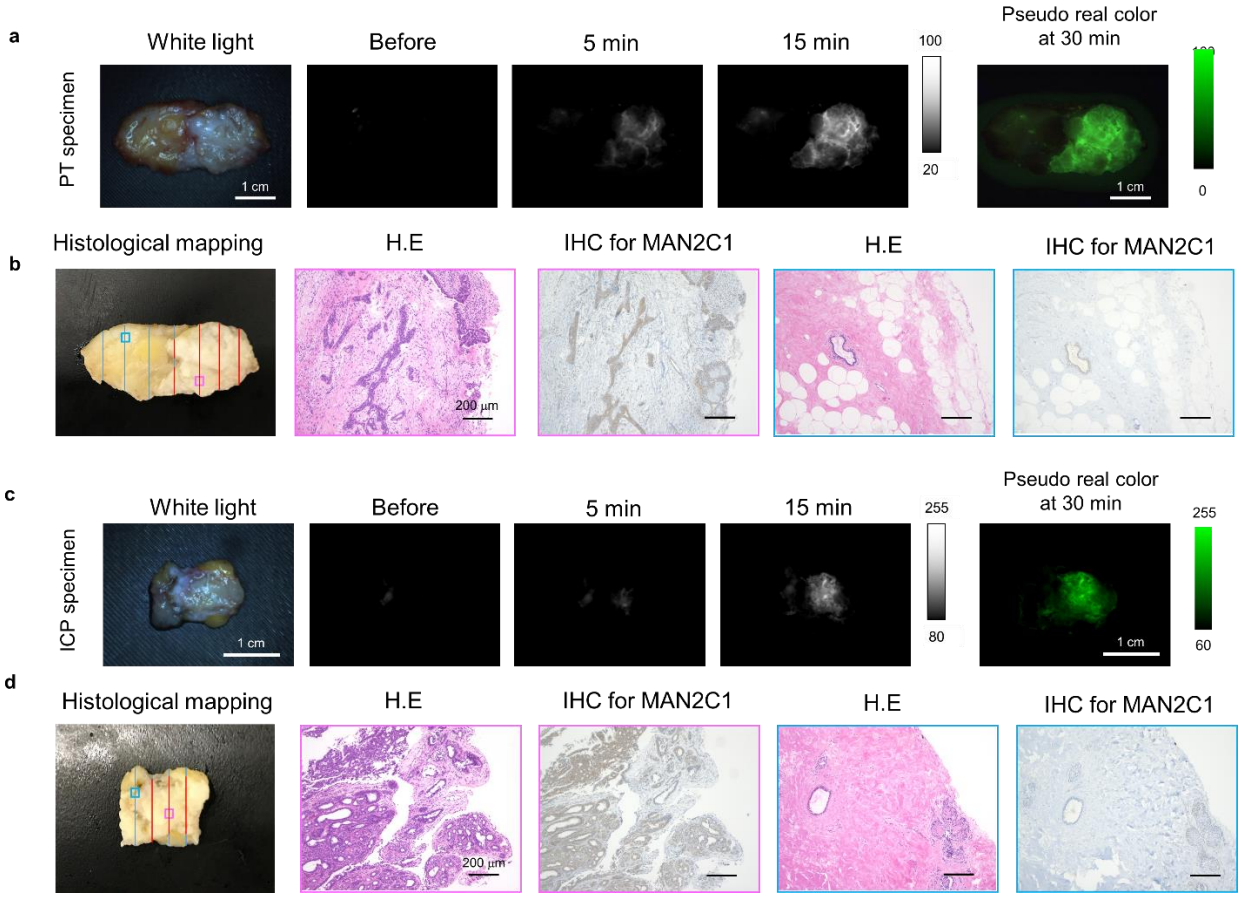

Figure S12. Evaluation of probe HMRef-αMan in surgically resected fresh PT and ICP tissues from human breast. (**a**) Time-dependent fluorescence image of surgically resected fresh human PT specimens containing both normal and benign tissues after administration of HMRef-αMan. Probe solution was prepared with PBS (-) containing 0.5 *v*/*v* % DMSO as a co-solvent. [HMRef-αMan] = 50 μM. Scale bar, 1 cm. (**b**) Histological mapping of the specimen: red lines show PT and blue lines show no tumor (left). Histological analysis and IHC analysis for MAN2C1 of boxed regions with strong fluorescence activation (pink box) or with no fluorescence activation (blue box). Scale bar, 200 μm. (**c**) Time-dependent fluorescence image of surgically resected fresh human ICP specimens containing both normal and benign tissues after administration of HMRef-αMan. Probe solution was prepared with PBS (-) containing 0.5 *v*/*v* % DMSO as a co-solvent. [HMRef-αMan] = 50 μM. Scale bar, 1 cm. (**d**) Histological mapping of the specimen: red lines show ICP and blue lines show no tumor (left). Histological analysis and IHC analysis for MAN2C1 of boxed regions with strong fluorescence activation (pink box) or with no fluorescence activation (blue box). The IHC image of IDP are the same image shown in **Figure 5** (**a**). Scale bar, 200 μm.

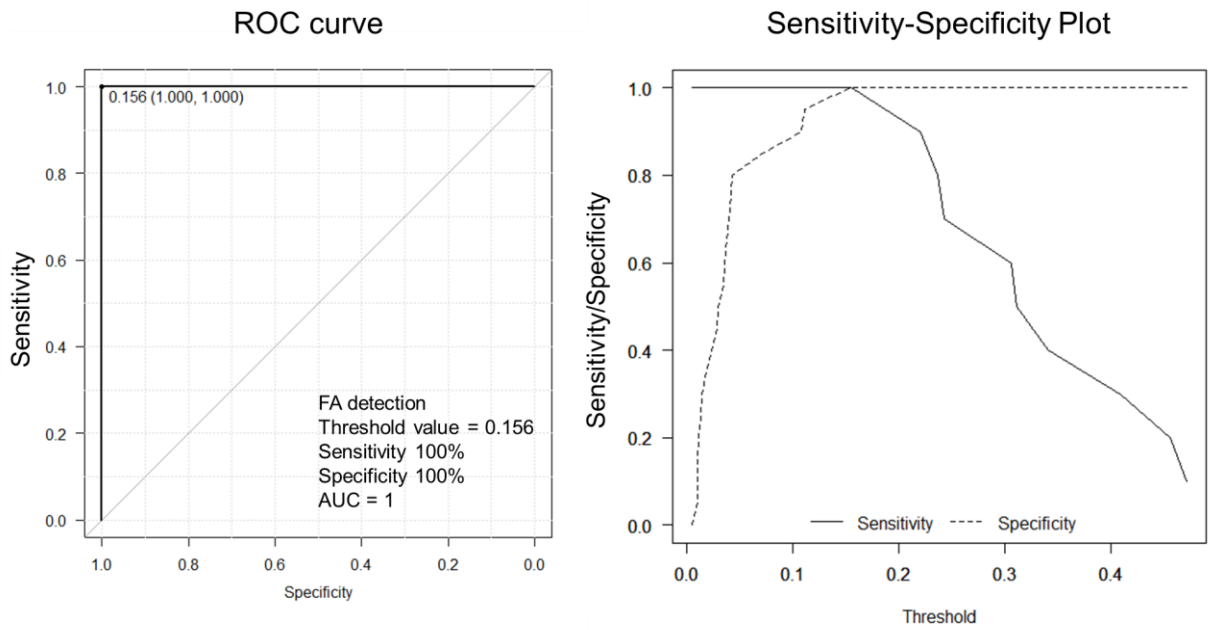

Figure S13. ROC curves and Sensitivity-Specificity plots for FA detection. Threshold value, sensitivity, specificity and AUC of HMRef-αMan in FA detection were evaluated from the receiver operating characteristic curve (N = 20 for normal, N = 10 for FA).

Table S3. List of detected proteins in DEG assay of a human FA surgical specimen. 104 proteins were identified by peptide mass fingerprinting analysis. MAN2C1 (also known as α-mannosidase 6A8B) is highlighted in yellow.

	Identified Proteins (104)	Molecular Weight	Protein Identification Probability
1	beta-filamin [Homo sapiens]	278 kDa	100%
2	fibronectin 1, isoform CRA_h [Homo sapiens]	256 kDa	100%
3	fatty acid synthase [Homo sapiens]	273 kDa	100%
4	talin-1 [Homo sapiens]	271 kDa	100%
5	tenascin X [Homo sapiens]	464 kDa	100%
6	filamin-A isoform 2 [Homo sapiens]	281 kDa	100%
7	beta-spectrin [Homo sapiens]	275 kDa	100%
8	keratin, type I cytoskeletal 9 [Homo sapiens]	62 kDa	100%
9	Keratin 10 [Homo sapiens]	59 kDa	100%
10	spectrin, alpha, non-erythrocytic 1 (alpha-fodrin) variant, partial [Homo sapiens]	288 kDa	100%
11	Keratin 8 [Homo sapiens]	54 kDa	100%
12	alpha-2-macroglobulin precursor [Homo sapiens]	163 kDa	100%
13	adenylyl cyclase-associated protein 1 isoform a [Homo sapiens]	52 kDa	100%
14	Chain A, Structure Of Human Apolactoferrin At 2.0 A Resolution.	76 kDa	100%
15	Chain B, Quantitative Interaction Mapping Reveals An Extend ed Ubiquitin Regulatory Domain In Aspl That Disrupts Functional P97 Hexamers And Induces Cell Death	89 kDa	100%
16	40-kDa keratin protein, partial [Homo sapiens]	44 kDa	100%
17	ATP:citrate lyase [Homo sapiens]	121 kDa	100%
18	epidermal cytokeratin 2 [Homo sapiens]	66 kDa	100%
19	Homo sapiens lamin A/C, partial [synthetic construct]	65 kDa	100%
20	Chain A, Crystal Structure Of Recombinant Human Triosephosphate Iso merase At 2.8 Angstroms Resolution. Triosephosphate Isomerase Related Human Genetic Disorders And Comparison With The Trypanosomal Enzyme	27 kDa	100%
21	Keratin 18 [Homo sapiens]	48 kDa	100%
22	plectin 1, intermediate filament binding protein 500kDa, isoform CRA_c [Homo sapiens]	290 kDa	100%
23	Keratin 7 [Homo sapiens]	51 kDa	100%
24	Homo sapiens actinin, alpha 1, partial [synthetic construct]	103 kDa	100%
25	TGFBI, partial [synthetic construct]	75 kDa	100%
26	Chain A, Crystal structure of smooth muscle G actin DNase I complex	42 kDa	100%
27	Chain A, Complex of APLF factor and Ku heterodimer bound to DNA	63 kDa	100%
28	hypothetical protein EGM_12944, partial [Macaca fascicularis]	281 kDa	100%
29	PREDICTED: keratin, type I cytoskeletal 16 isoform X1 [Mandrillus leucophaeus]	92 kDa	100%
30	Chain B, Crystal Structure of the Ku Heterodimer	64 kDa	100%
31	Chain A, Crystal structure of phosphorylated mutant of glycerald ehyde 3-phosphate dehydrogenase from human placenta at 3.15A resolution	36 kDa	100%
32	complement component C3 [Homo sapiens]	187 kDa	100%
33	Keratin 6A [Homo sapiens]	60 kDa	100%
34	keratin 1 [Homo sapiens]	66 kDa	100%
35	Membrane-organizing extension spike protein, partial [Macaca mulatta]	67 kDa	100%
36	IGHA1, partial [synthetic construct]	53 kDa	100%
37	decorin, partial [synthetic construct]	40 kDa	100%
38	elongation factor Tu [Mus musculus]	50 kDa	100%
39	Chain 4, Structure Of The 80s Mammalian Ribosome Bound To Ee f2 (this Entry Contains The Large Ribosomal Subunit Proteins)	95 kDa	100%
40	heat shock protein 70 [Megalobrama amblycephala]	71 kDa	100%
41	PREDICTED: phosphatidylinositol transfer protein beta isoform-like isoform X1 [Colobus angolensis palliatus]	32 kDa	100%
42	alpha actinin 4 [Homo sapiens]	102 kDa	100%
43	PREDICTED: dynactin subunit 1 isoform X6 [Gorilla gorilla gorilla]	139 kDa	100%
44	Chain A, Structure Of Human Placental S-adenosylhomocysteine Hydrolase: D etermination Of A 30 Selenium Atom Substructure From Data At A Single Wavelength	47 kDa	100%
45	vimentin [Homo sapiens]	54 kDa	100%
46	unnamed protein product [Homo sapiens]	53 kDa	100%
47	Rho-associated, coiled-coil containing protein kinase 1 [Homo sapiens]	158 kDa	100%
48	Chain A, Structure Of Human Glutamate Dehydrogenase-Apo Form	56 kDa	100%

49	keratin 5 [Homo sapiens]	62 kDa	100%
50	Chain A, Human Muscle L-lactate Dehydrogenase M Chain, Ternary Complex W ith Nadh And Oxamate	37 kDa	100%
51	Chain A, Crystal Structure Of Human Serum Albumin	66 kDa	100%
52	Ig alpha-2 chain - human (fragment)	37 kDa	100%
53	beta-actin [Neovison vison]	42 kDa	100%
54	PREDICTED: LOW QUALITY PROTEIN: pre-mRNA-processing factor 19, partial [Acanthisitta chloris]	53 kDa	100%
55	Chain A, Crystal Strucutre Of Udp-Glucose Pyrophosphorylase Of Homo Sapiens	59 kDa	100%
56	alpha mannosidase 6A8B [Homo sapiens]	118 kDa	100%
57	tenascin C (hexabrachion), isoform CRA_a [Homo sapiens]	241 kDa	100%
58	filamin, alpha (predicted), isoform CRA_b [Rattus norvegicus]	277 kDa	100%
59	Chain L, CRYSTAL STRUCTURE OF A CHIMERIC FAB' FRAGMENT OF AN ANTIBODY BINDING TUMOUR CELLS	23 kDa	100%
60	Chain C, Solution Structure Of Human Immunoglobulin M	57 kDa	100%
61	beta-actin, partial [Falco peregrinus]	15 kDa	100%
62	Chain A, Crystal structure of human Gelsolin domains G1-G3 bound to Actin	42 kDa	100%
63	Chain A, Structure Of Human Liver Chichi Alcohol Dehydrogenase (A Glutathione-Dependent Formaldehyde Dehydrogenase)	40 kDa	100%
64	extracellular matrix protein periostin-bm [Homo sapiens]	87 kDa	100%
65	tenascin isoform X5 [Homo sapiens]	231 kDa	100%
66	keratin 15, partial [synthetic construct]	49 kDa	100%
67	Chain E, Leech-Derived Tryptase InhibitorTRYPSIN COMPLEX	23 kDa	100%
68	filaggrin-2 [Homo sapiens]	248 kDa	100%
69	Chain A, Solution Structure Of Double Super Helix Model	28 kDa	100%
70	Chain A, Artificial Mutant (Alpha Y42h) Of Deoxy Hemoglobin	15 kDa	100%
71	AAA ATPase [Wallemia mellicola CBS 633.66]	90 kDa	100%
72	hypothetical protein EGK_03743 [Macaca mulatta]	11 kDa	99%
73	actin, partial [Ghelna canadensis]	26 kDa	97%
74	PREDICTED: cationic trypsin-3 [Marmota marmota marmota]	26 kDa	97%
75	Threonyl-tRNA synthetase, cytoplasmic, partial [Anas platyrhynchos]	82 kDa	94%
76	keratin, type II cytoskeletal 1 [Pongo abelii]	66 kDa	100%
77	PREDICTED: keratin, type I cytoskeletal 15 [Propithecus coquereli]	49 kDa	99%
78	PREDICTED: anionic trypsin-1 [Jaculus jaculus]	26 kDa	98%
79	beta actin, partial [Dasyatis akajei]	35 kDa	97%
80	PREDICTED: actin-5C-like [Rhagoletis zephyria]	42 kDa	96%
81	hypothetical protein BOX15_Mlig026283g2 [Macrostomum lignano]	88 kDa	96%
82	cell division control protein 48 aaa family protein (transitional endoplasmic reticulum atpase),putative [Schistosoma mansoni]	89 kDa	94%
83	actin, partial [Habronattus americanus]	28 kDa	92%
84	Chain A, Crystal Structure Of Sept2 G-Domain	36 kDa	90%
85	Peripherin [Myotis brandtii]	66 kDa	90%
86	ribosomal protein L10 [Homo sapiens]	24 kDa	80%
87	polyposis locus-encoded protein [Homo sapiens]	21 kDa	78%
88	PREDICTED: supervillin [Nanorana parkeri]	260 kDa	78%
89	Chain A, Crystal Structure Of The Mouse Cavin1 Hr1 Domain	12 kDa	78%
90	beta-actin, partial [Oryzias dancena]	32 kDa	76%
91	HLH domain-containing protein [Oryctes borbonicus]	264 kDa	76%
92	plectin isoform X1 [Carlito syrichta]	534 kDa	75%
93	keratin, type II cytoskeletal 75 [Mus pahari]	118 kDa	73%
94	Chain E, Complex Of Eeti-Ii With Porcine Trypsin	24 kDa	71%
95	beta-actin, partial [Gobio gobio]	17 kDa	69%
96	hypothetical protein AB205_0198390, partial [Rana catesbeiana]	47 kDa	64%
97	periodontal ligament-specific periostin [Homo sapiens]	84 kDa	62%
98	Chain A, Solution structure of the SEA domain of human mucin 1 (MUC1)	8 kDa	32%
99	Zgc:73317 [Danio rerio]	51 kDa	28%
100	PREDICTED: threonine--tRNA ligase, cytoplasmic [Clupea harengus]	83 kDa	13%
101	PREDICTED: keratin, type I cytoskeletal 19-like, partial [Hipposideros armiger]	30 kDa	4%
102	actin, partial [Talavera minuta]	22 kDa	4%
103	hypothetical protein cypCar_00032676, partial [Cyprinus carpio]	91 kDa	0%
104	hypothetical protein A6R68_16192 [Neotoma lepida]	48 kDa	0%

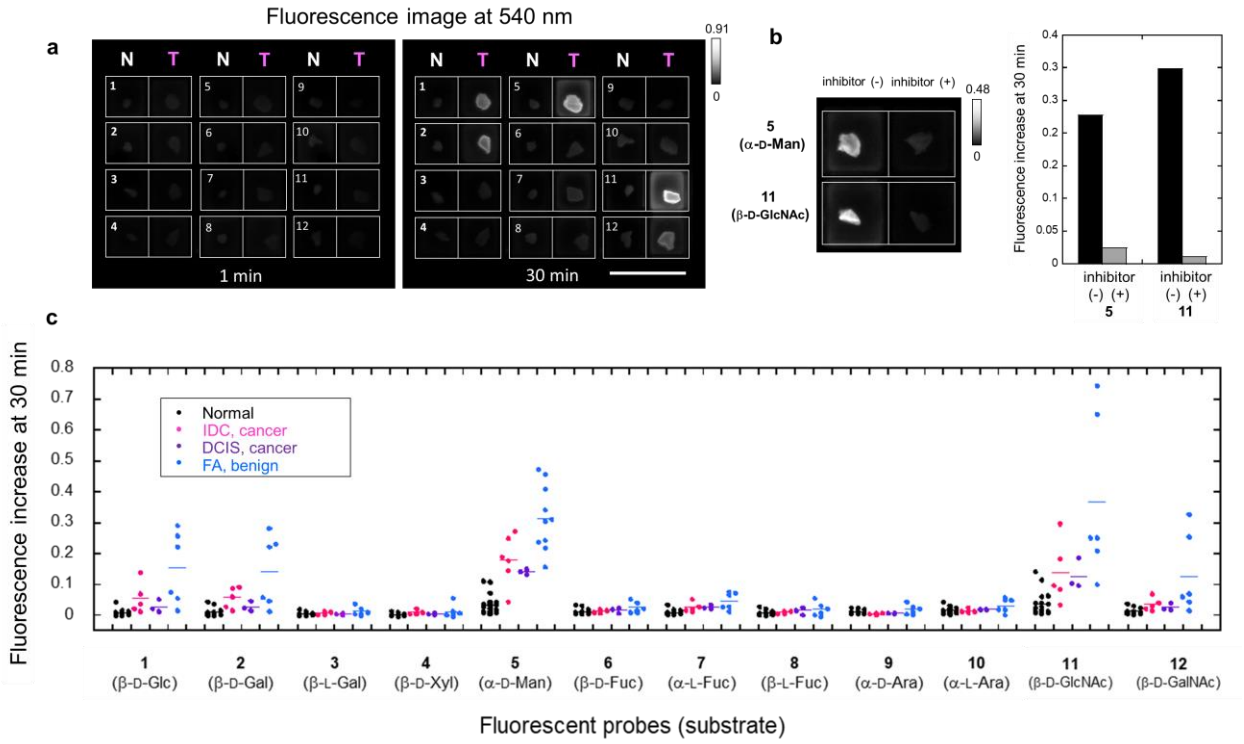

Figure S14. Comparison of fluorescence increase in normal, cancer and FA (benign) breast specimens. (**a**) Example of screening using surgically resected frozen human breast FA and normal tissues. The compound number of the applied probe is shown on each well. Probe solution was prepared with PBS (-) containing 0.5 *v*/*v* % DMSO as a co-solvent. [fluorescent probe] = 50 μM. (**b**) Fluorescence increase at 30 min in breast FA tissues in the presence and absence of each inhibitor. Black bars: fluorescence increase in the absence of inhibitor. Gray bars: the fluorescence increase in the presence of inhibitor. [fluorescent probe] = 50 μM, [swainsonine] = 500 μM for probe **5** (HMRef-αMan), [PUGNAc] = 500 μM for probe **11** (β-D-GlcNAc). (**c**) Comprehensive analysis of intact glycosidase activities in normal breast, IDC, DCIS and FA tissues using 12 fluorescent probes. Fluorescence increase represents the increase at 30 min from 1 min after addition of fluorescent probes. Black, pink, purple and blue dots represent fluorescence increase in normal, IDC, DCIS and FA tissues, respectively. For probe **5** (HMRef-αMan), normal (N = 20), IDC (N = 7), DCIS (N = 3) and FA (N = 10) tissues were examined. For other probes, normal (N = 14), IDC (N = 5), DCIS (N = 3) and FA (N = 6) tissues were examined. Plots of normal, IDC and DCIS contain the same values as shown in **Figure 3** (**d**). [fluorescent probe] = 50 μM.

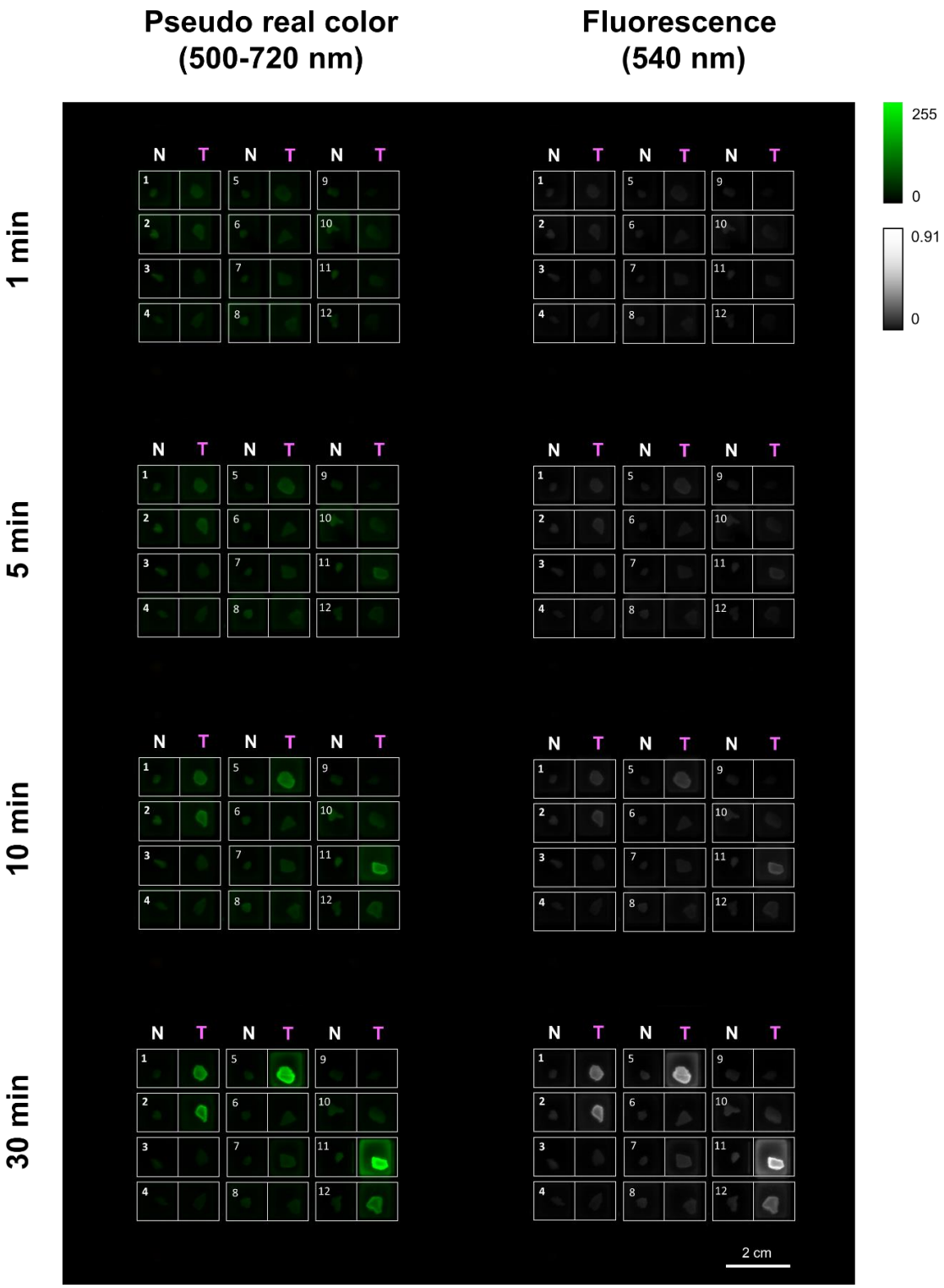

Figure S15. Example of screening with surgically resected normal and FA tissues from human breast. Exposure time = 100 msec (1-10 min), 60 msec (30 min), [fluorescent probe] = 50 μM. Scale bar, 2 cm.

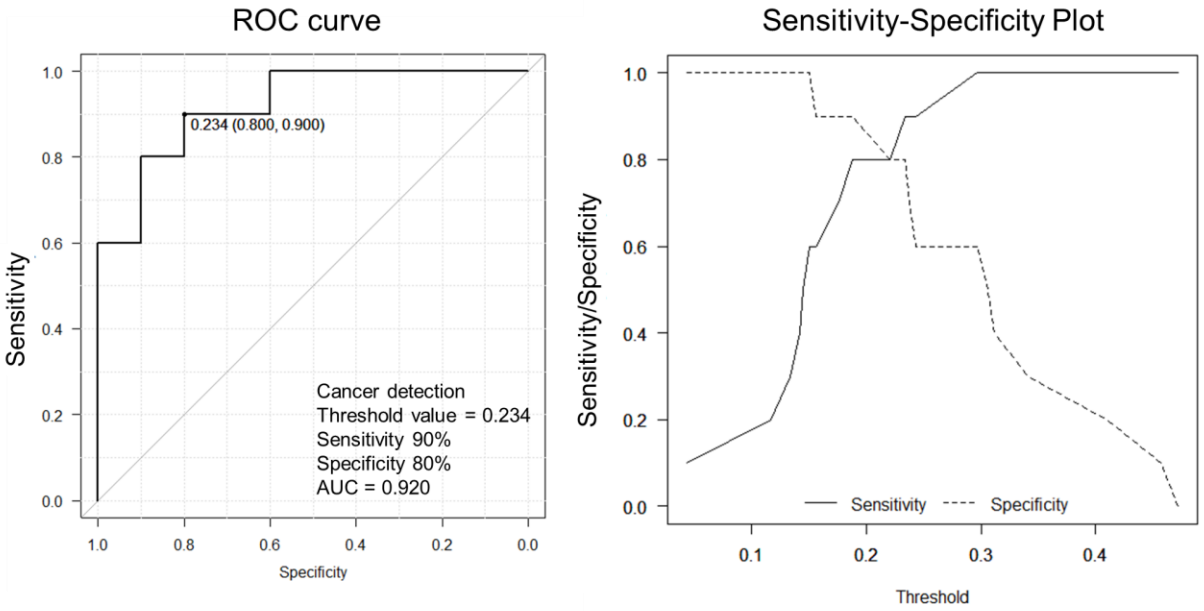

Figure S16. ROC curve and sensitivity-specificity plot for binary classification (cancer/FA) by HMRef-αMan. Threshold value, sensitivity, specificity and AUC of each probe were evaluated from the receiver operating characteristic curve. Breast cancer (N = 7 for IDC, N = 3 for DCIS) and FA (N = 10) tissues were examined.

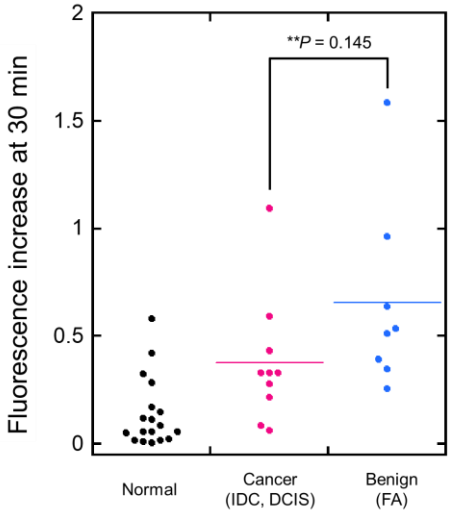

Figure S17. Fluorescence increases of gGlu-HMRG in normal, cancer (IDC and DCIS) and benign (FA) tissues from human breast. Plots of normal, IDC and DCIS contain the same values as shown in **Figure 3** (**d**). *P* = 0.145 by Welch's *t*-test (N = 19 for normal, N = 7 for IDC, N = 3 for DCIS, N = 8 for FA). [gGlu-HMRG] = 50 μM.

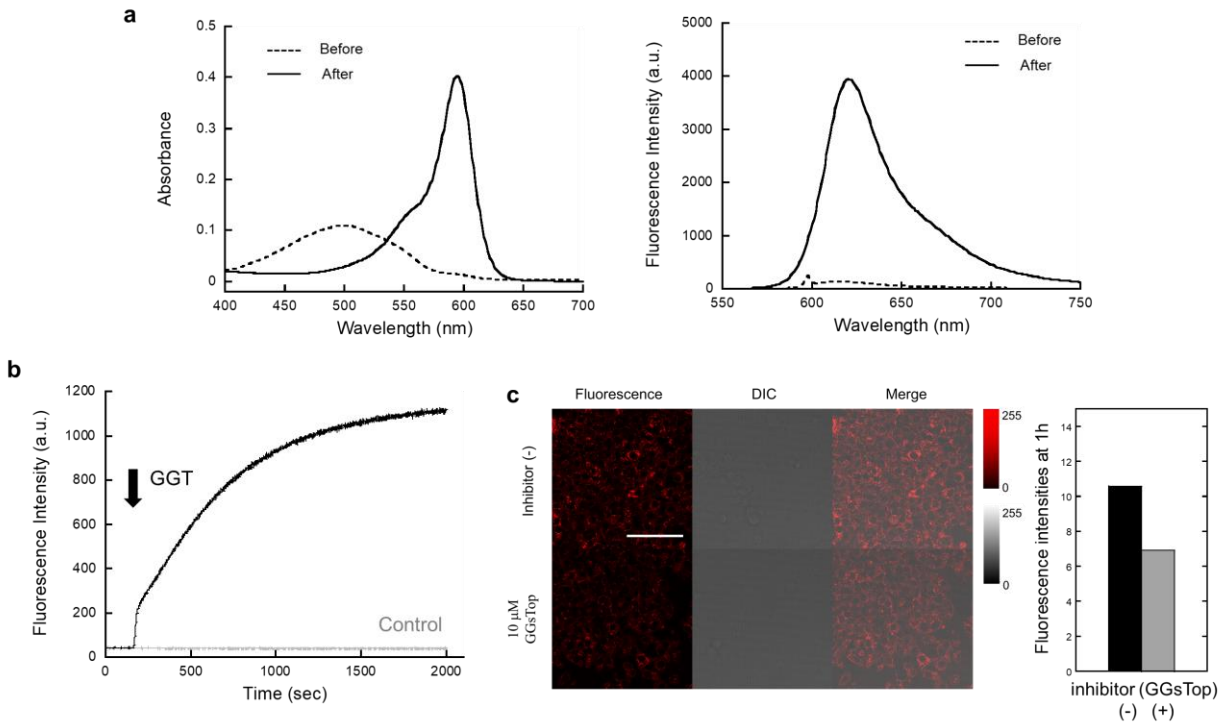

Figure S18. Red fluorescent probe for GGT activity. (**a**) Absorption (left) and fluorescence (right) spectra of gGlu-2OMe SiR600 before and after reaction with GGT. (**b**) The time course of fluorescence intensity of gGlu-2OMe SiR600 upon addition of GGT was monitored at excitation/emission wavelengths of 595 nm/615 nm. To a 10 μM solution of gGlu-2OMe SiR600 in 3 mL of PBS (-), pH 7.4, containing 0.1% DMSO as a cosolvent, GGT (Oriental Yeast Co., Ltd., 50 units) was added at 150 s. The gray line (control) shows the fluorescence change in the absence of GGT. (**c**) Confocal images of fluorescence intensity in GGT-positive SHIN3 cells[1] treated with gGlu-2OMe SiR600 for 1 h in the presence and absence of GGsTop (left). Fluorescence intensity of SHIN3 cells at 1 h (right). Black bar: fluorescence intensity in the absence of GGsTop. Gray bar: fluorescence intensity in the presence of GGsTop. Ex/Em = 593 nm/600-800 nm. [gGlu-2OMe SiR600] = 1 μM, [GGsTop] = 10 μM. Scale bar, 100 μm.

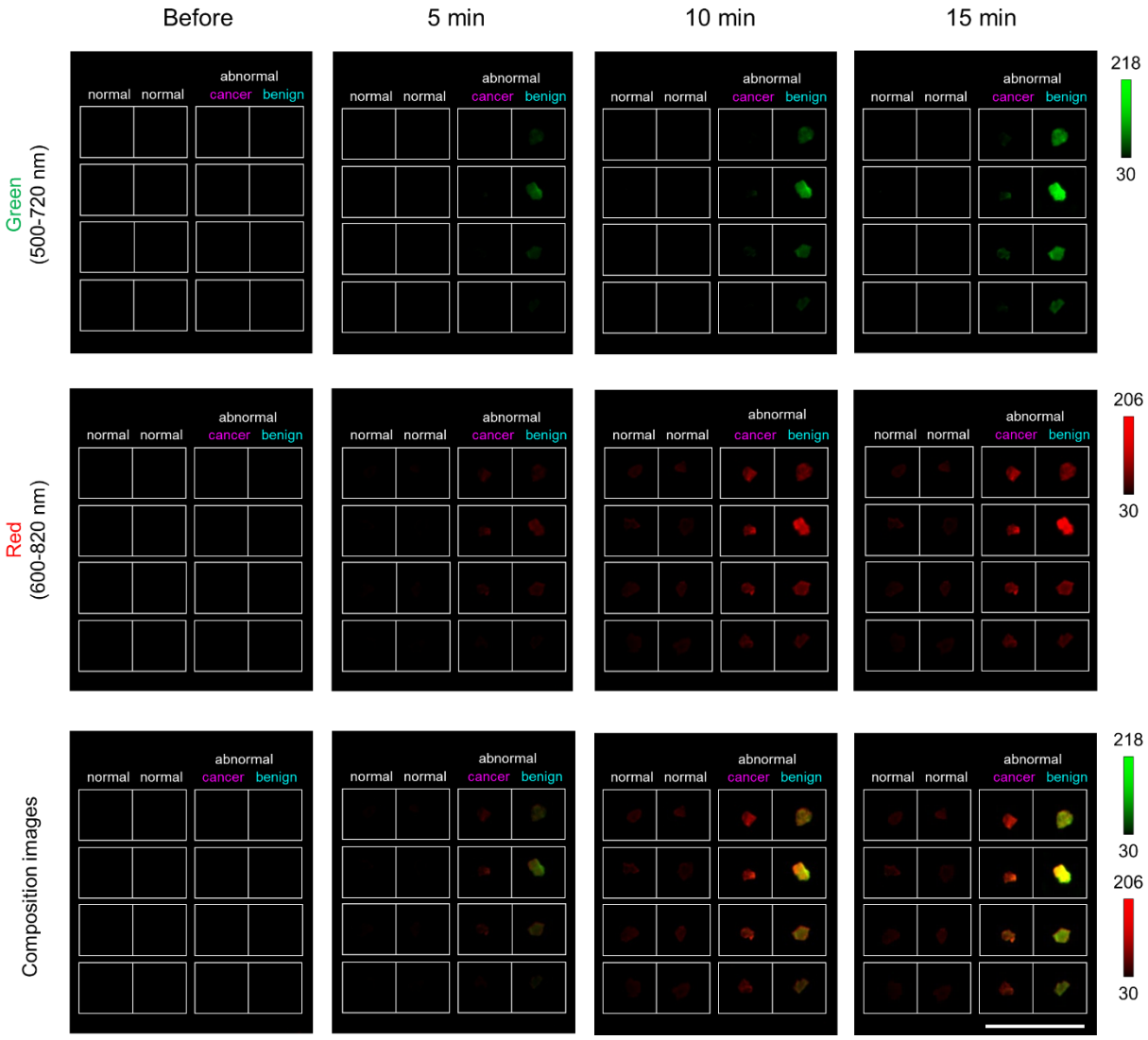

Figure S19. Time-dependent fluorescence images of human normal, cancer and benign (FA) tissues from human breast after administration of HMRef-αMan and gGlu-2OMe SiR600. Green channel: pseudo real color image at 500-720 nm. Red channel: pseudo real color image at 600-820 nm. Scale bar, 2 cm.

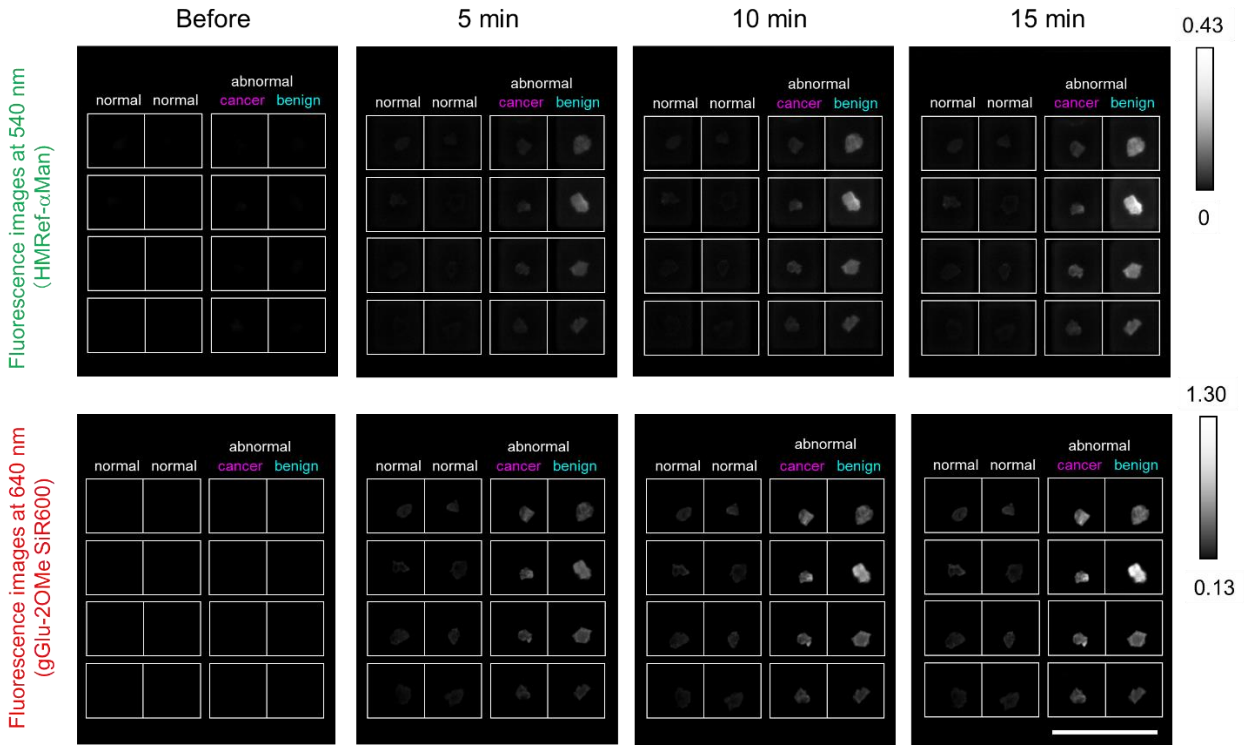

Figure S20. Time-dependent fluorescence images at 540 nm and 640 nm of normal, cancer and benign (FA) tissues from human breast after administration of HMRef-αMan and gGlu-2OMe SiR600. Fluorescence at 540 nm is due to the HMRef fluorophore. Fluorescence at 640 nm is due to the 2OMe SiR600 fluorophore. Scale bar, 2 cm.

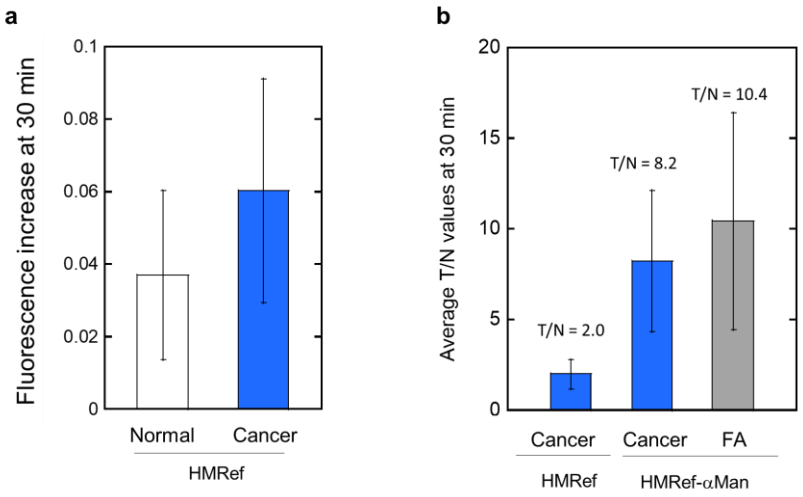

Figure S21. Fluorescence increase of breast cancer and normal tissues in the presence of HMRef or HMRef-αMan. (**a**) Fluorescence increases of normal and IDC tissues from human breast in the presence of HMRef fluorophore. White bar: fluorescence increase in normal tissues (N = 4) from different patients. Blue bar: fluorescent increase in cancer (IDC) tissues (N = 4) from different patients. Fluorescence increase was measured at 30 min after administration of HMRef. The average tumor/non-tumor ratio (T/N) was 2.0, from which we can infer that observed T/N values over 2.0 represent differences of enzyme activity between tumor and non-tumor tissues. Error bars represent s.d. [HMRef] = 1 μM. (**b**) T/N values at 30 min in breast cancer (IDC and DCIS) and benign FA tissues. Average T/N values obtained with HMRef-αMan in breast cancer and benign FA were 8.2 and 10.4, respectively. For HMRef-αMan, breast IDC (N = 7), DCIS (N = 3) and FA (N = 10) tissues were evaluated. T/N values with HMRef-αMan were calculated using the fluorescence increase values shown in **Figure 5** (**a**). Error bars represent s.d. [HMRef-αMan] = 50 μM.

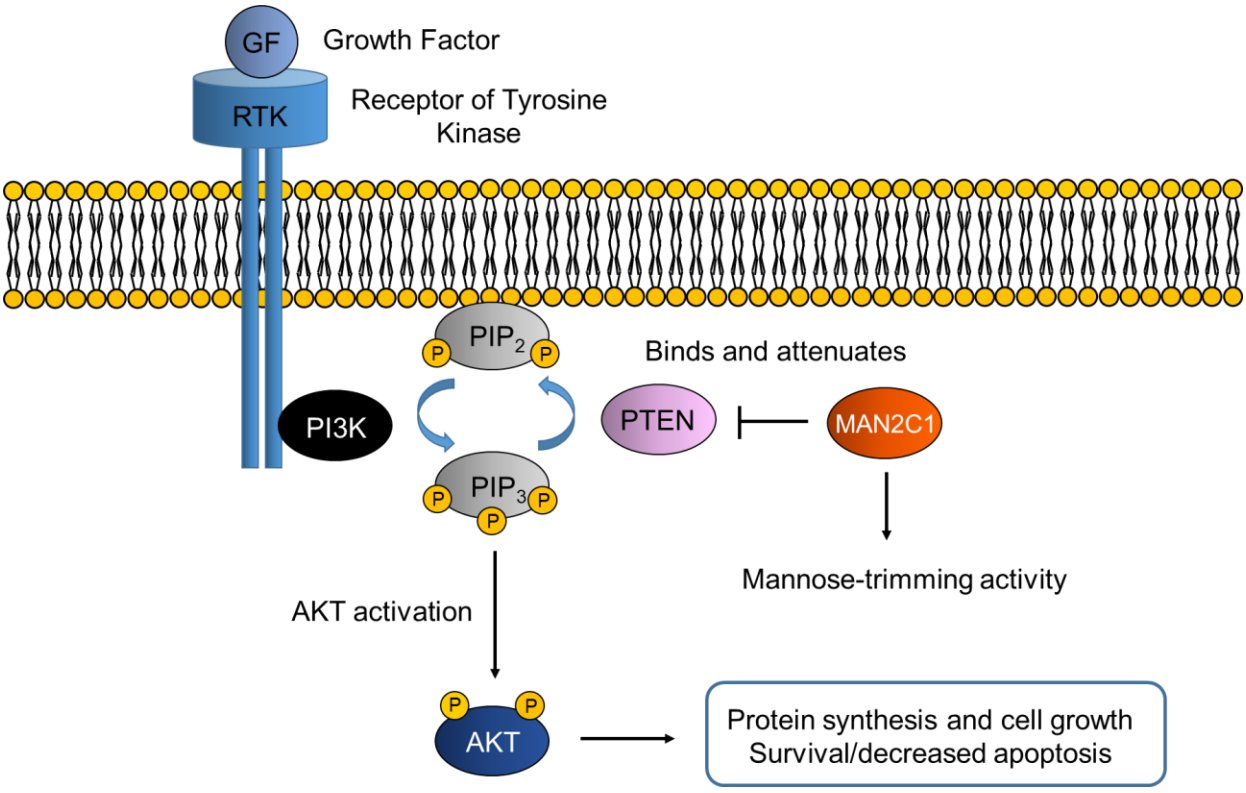

Figure S22. MAN2C1 attenuates PTEN function. He *et al.* reported that inactivation of PTEN by MAN2C1 leads to activation of the PI3K/AKT pathway in PTEN-positive prostate cancer. They also demonstrated that MAN2C1 siRNA reduced AKT activation in PTEN-positive DU145 prostate cancer cells, as well as in MCF7 breast cancer cells.[3] MAN2C1 may function similarly in clinical breast cancer specimens, as shown in **Figure S21**.

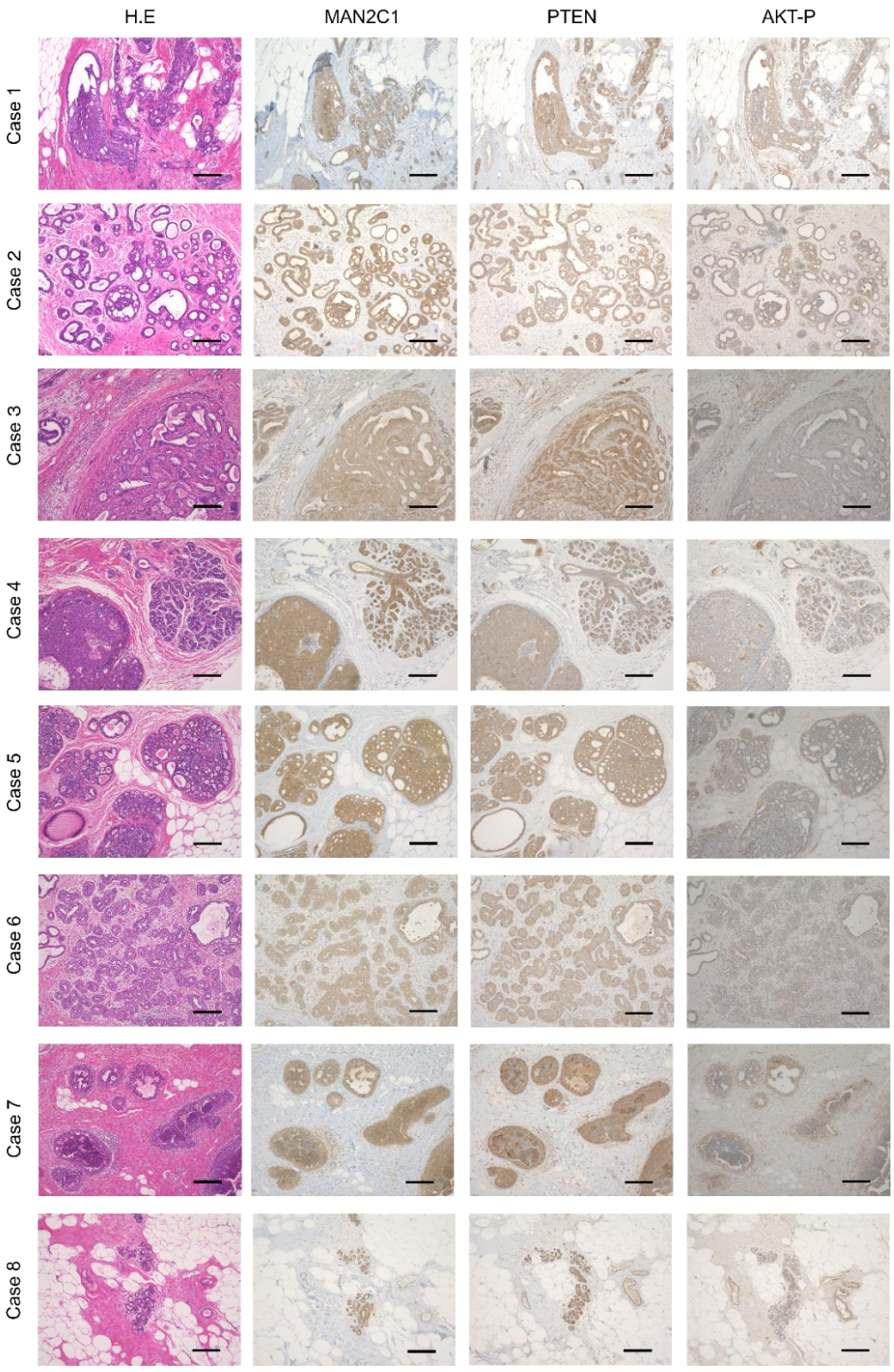

Figure S23. H.E and IHC staining of DCIS tissue from 8 different patients. Co-expression of MAN2C1, PTEN and AKT-P (pSer473) was observed in all human DCIS tissues evaluated in this experiment. This feature is similar to the case of PTEN-positive prostate cancer. Scale bar, 200 μm.

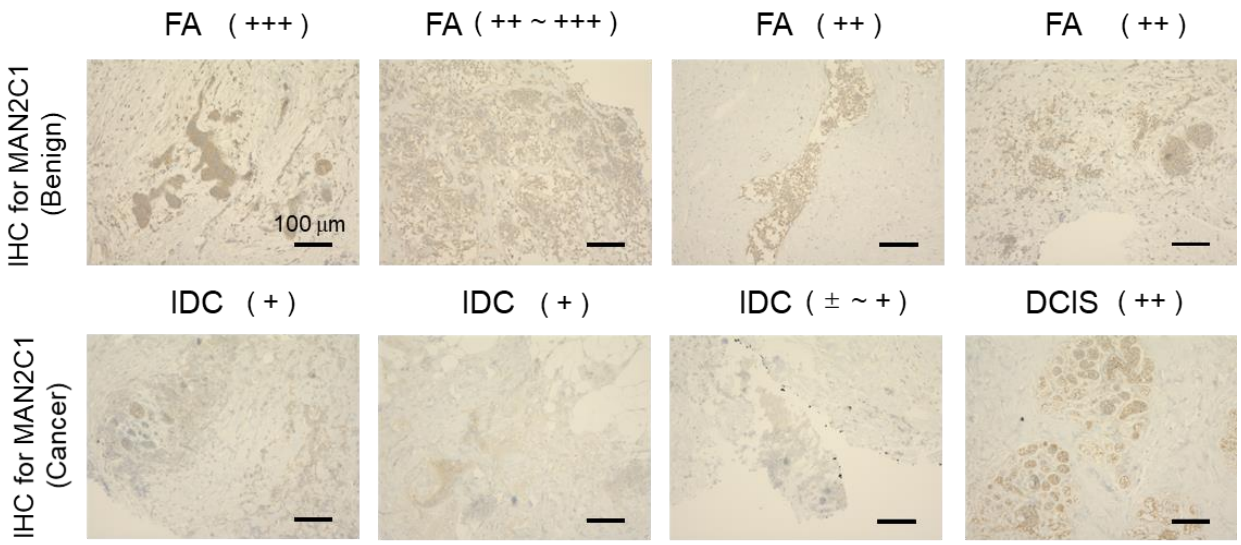

Figure S24. IHC staining of benign FA and cancer tissues. Expression levels of MAN2C1 at the tumor regions in the specimens in **Figure 6** (**c**) were evaluated in terms of IHC by means of visual scoring by a pathologist (negative "-", weak "+", medium "++", and strong "+++" positive staining). Scores are shown in above each IHC image. Levels of MAN2C1 tend to be higher in benign FA tissues than in cancerous tissues in this experiment. Scale bar, 100 μm.

Organic synthesis and characterization of compounds.

HMRef was synthesized according to **Scheme 1**.

Scheme 1. Synthesis of HMRef fluorophore

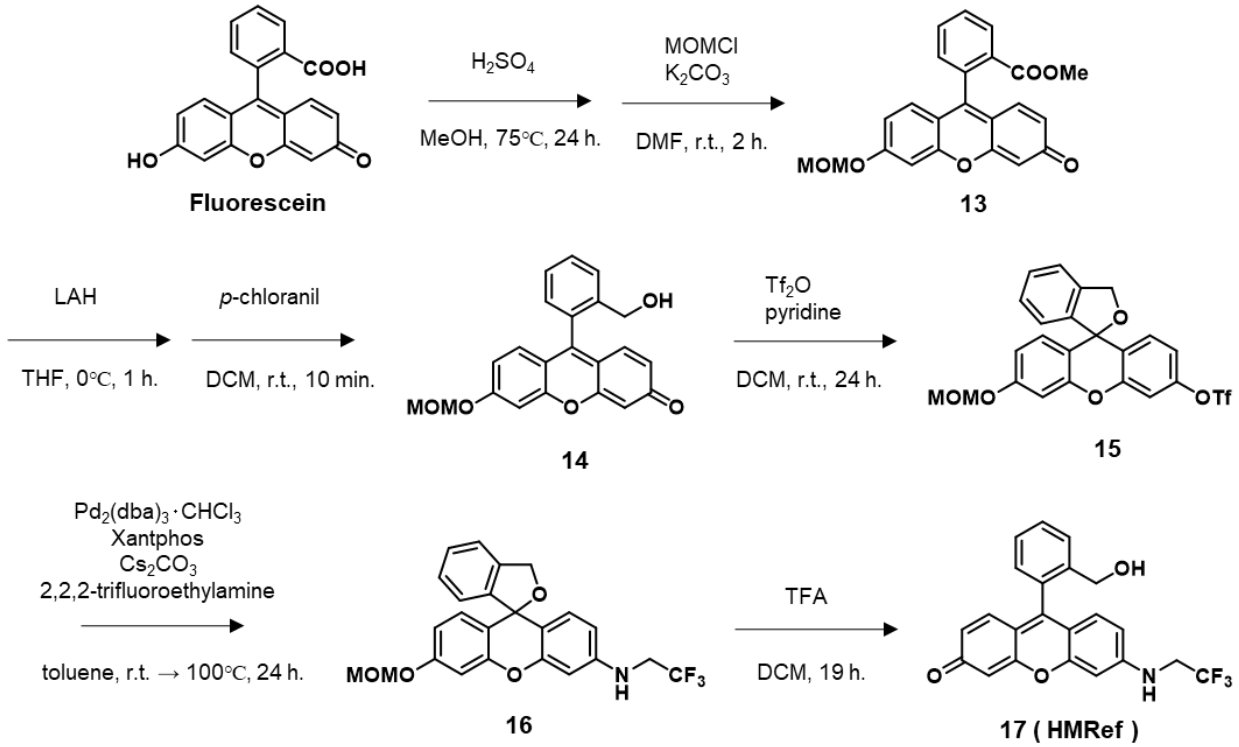

Procedure for the synthesis of 13. A mixture of fluorescein (10.0 g, 30.1 mmol) and H_2SO_4 (20.0 mL) in 100 mL dried MeOH was stirred for 24 h at 80 °C. The solution was concentrated under reduced pressure and neutralized with sat. aq. $NaHCO_3$. The product was collected by suction filtration, washed with water several times, and extracted with MeOH. The solution was concentrated under reduced pressure to afford an orange-red powder. A mixture of this product, chloromethyl methyl ester (8.48 g, 105 mmol) and K_2CO_3 (20.0 g, 144 mmol) in 100 mL dried DMF was stirred for 24 h at room temperature. The solution was concentrated under reduced pressure to remove DMF. To the residue were added DCM and 15.0 mL of sat. aq. NH_4Cl. The mixture was stirred for 10 min, then the aqueous layer was acidified to pH ~3 with 85% phosphoric acid, and the organic layer was isolated. The DCM extracts were washed with brine, dried over Na_2SO_4, and filtered. Silica gel 60 was added to the filtrate. After evaporation to dryness, the resulting slurry was applied to a column of silica gel 60 and eluted with ethyl acetate : hexane = 4 : 1 solvent to afford **13** as a yellow powder (11.51 g, 29.5 mmol) in 97.9 % yield. The identity of the product was confirmed by means of ^{1}H NMR, ^{13}C NMR and ESI-HRMS. ^{1}H NMR (400 MHz, CD_3OD): δ 8.23 (d, *J* = 1.2 Hz, 1H), 7.88 (t, *J* = 1.2 Hz, 1H), 7.749-7.39 (m, 12H), 7.16 (d, *J* = 7.2 Hz, 1H), 6.60-6.56 (m, 6H), 1.08 (s, 18H). ^{13}C NMR (101 MHz, CD_3OD): δ 183.9, 165.1, 161.0, 158.3,

153.1, 149.8, 133.8, 133.2, 130.7, 130.4, 130.0, 129.5, 128.9, 117.0, 115.0, 114.4, 102.7, 94.1, 56.1, 52.3. ESI-HRMS (ESI +) m/z calcd. for $[M+H]^+$, 391.11761; found, 391.11690.

Procedure for the synthesis of 14. A mixture of **13** (11.5 g, 29.5 mmol) and LAH (800 mg, 21.1 mmol) in 150 mL dried THF was stirred for 2 h in an ice bath. The reaction was quenched by the addition of MeOH, and the mixture was concentrated under reduced pressure. After the addition of Rochelle salt aq. and AcOEt, the whole was stirred for 1 h at room temperature. The organic layer was washed with water and brine, dried over Na_2SO_4, and evaporated. The residue was dissolved in 100 mL CH_2Cl_2. To this solution, *p*-cloranil (3.20 g, 13.0 mmol) was added, and the mixture was stirred for 10 min at room temperature. The reaction was quenched by the addition of silica gel 60, and the mixture was evaporated to dryness. The resulting slurry was subjected to flash column chromatography (CH_2Cl_2 : MeOH = 95 : 5) to afford **14** as a yellow powder (5.97 g, 16.5 mmol) in 55.9 % yield. The identity of the product was confirmed by means of ESI-HRMS. ESI-HRMS (ESI +) m/z calcd. for $[M+H]^+$, 363.12270; found, 363.12286.

Procedure for the synthesis of 15. A mixture of **14** (5.97 g, 16.5 mmol), Tf_2O (5.80 mL, 30.5 mmol) and pyridine (5.80 mL, 72.0 mmol) in 150 mL dried CH_2Cl_2 was stirred for 24 h at room temperature, and then evaporated. The residue was purified by flash column chromatography using CH_2Cl_2 as the eluent to obtain **15** (4.46 g, 9.02 mmol) as a light yellow oil in 54.7% yield. The identity of the product was confirmed by means of ^{1}H NMR, ^{13}C NMR and ESI-HRMS. ^{1}H NMR (400 MHz, CD_2Cl_2): δ 7.41-7.45 (m, 2H), 7.30-7.34 (m, 1H), 7.22 (d, *J* = 2.4 Hz, 1H), 7.15 (d, *J* = 8.4 Hz, 1H), 6.71 (dd, *J* = 2.2 Hz, 8.8 Hz, 1H), 7.01 (dd, *J* = 2.4 Hz, 8.8 Hz, 1H), 6.96-6.98 (m, 2H), 6.91 (d, *J* = 7.6 Hz, 1H), 6.81 (dd, *J* = 2.4 Hz, 8.8 Hz, 1H), 5.39 (s, 2H), 5.36 (d, *J* = 1.2 Hz, 1H), 5.23 (s, 2H), 3.49 (s, 3H). ^{13}C NMR (101 MHz, CD_2Cl_2): δ 158.5, 151.4, 151.0, 149.5, 145.0, 139.1, 131.1, 130.0, 128.9, 126.1, 123.8, 121.4, 118.3, 117.5, 116.6, 113.5, 110.2, 103.6, 94.9, 83.2, 73.2, 56.4. ESI-HRMS (ESI +) m/z calcd. for $[M+H]^+$, 495.07198; found, 495.06802.

Procedure for the synthesis of 16. Compound **15** (2.58 g, 5.22 mmol), $Pd_2(dba)_3 \cdot CHCl_3$ (1.87 g, 1.81 mmol), xantphos (610 mg, 1.05 mmol) and Cs_2CO_3 (4.26 g, 13.1 mmol) were dissolved in 50 mL dried toluene under an Ar atmosphere. 2,2,2-Trifluoroethylamine (3.00 mL) was added dropwise to the reaction solution with intensive stirring. Stirring was continued under an Ar atmosphere, first at room temperature for 30 min and then at 100°C for 24 h. The reaction mixture was allowed to cool to room temperature, diluted with CH_2Cl_2 and filtered through a Celite pad. After evaporation, the residue was purified by flash column chromatography (CH_2Cl_2 : MeOH = 99 : 1) to afford the desired product **16** (1.63 g, 3.68 mmol) as a slightly yellow powder in 70.2% yield. The identity of the product was confirmed by means of ^{1}H NMR, ^{13}C NMR and ESI-HRMS. ^{1}H NMR (400 MHz, $CDCl_3$): δ 7.26-7.36 (m, 2H), 7.24-7.28 (m, 1H), 6.91-6.88 (m, 2H), 6.84 (d, *J* = 8.8 Hz, 1H),

6.77 (d, *J* = 8.8 Hz, 1H), 6.71 (dd, *J* = 2.2 Hz, 8.8 Hz, 1H), 6.48 (d, *J* = 2.4 Hz, 1H), 6.37 (dd, *J* = 2.4 Hz, 8.4 Hz, 1H), 5.29 (s, 2H), 5.16 (s, 2H), 4.06 (t, *J* = 7.0 Hz, 1H), 3.65-3.80 (m, 2H), 3.47 (s, 3H). ^{13}C NMR (101 MHz, $CDCl_3$): δ 157.7, 151.7, 151.4, 147.2, 144.8, 139.4, 130.0, 129.8, 128.3, 128.0, 124.0, 120.6, 118.4, 115.4, 112.4, 109.9, 103.3, 99.2, 94.4, 83.5, 77.2, 56.1, 45.7 (q, *J* = 33.8 Hz). ESI-HRMS (ESI +) m/z calcd. for $[M+H]^+$, 444.14172; found, 444.14146.

Procedure for the synthesis of 17 (HMRef). Compound **16** (1.63 g, 3.67 mmol) was dissolved in 30.0 mL of CH_2Cl_2. TFA (10.0 mL) was added dropwise, and the reaction mixture was stirred at room temperature for 19 h. After dilution with CH_2Cl_2, the reaction solution was neutralized with 1 M NaOH, and washed with 1 M NaOH and brine. The organic layer was isolated, dried over Na_2SO_4, filtered, and concentrated to afford **17**, HMRef, (1.26 g, 3.15 mmol) as a red powder in 85.8 % yield. The identity of the product was confirmed by means of ^{1}H NMR and ESI-HRMS. ^{1}H NMR (400 MHz, CD_3OD + NaOD): δ 7.25-7.27 (m, 2H), 7.14-7.18 (m, 1H), 6.72 (d, *J* = 7.6 Hz, 1H), 6.51 (d, *J* = 8.8 Hz, 1H), 6.38 (d, *J* = 8.4 Hz, 1H), 6.35 (d, *J* = 2.4 Hz, 1H), 6.26-6.29 (m, 2H), 6.20 (dd, *J* = 2.4 Hz, 8.4 Hz, 1H), 3.71 (q, *J* = 9.3 Hz, 2H), 3.20-3.21 (m, 2H). ESI-HRMS (ESI +) m/z calcd. for $[M+H]^+$, 400.11605; found, 400.11436.

Purification of glycosidase-reactive probes by HPLC. Glycosidase-reactive probes synthesized according to **Schemes 2-13** were purified by reverse-phase HPLC (ODS column, 250 x 20 mm, pore size: 5 μm) with a gradient of 5-80% MeCN in water (0.1% TFA) over 90 min (flow rate; 1 mL / min, detection at 250 and 400 nm).

Scheme 2. Synthesis of probe **1** (β-D-Glc)

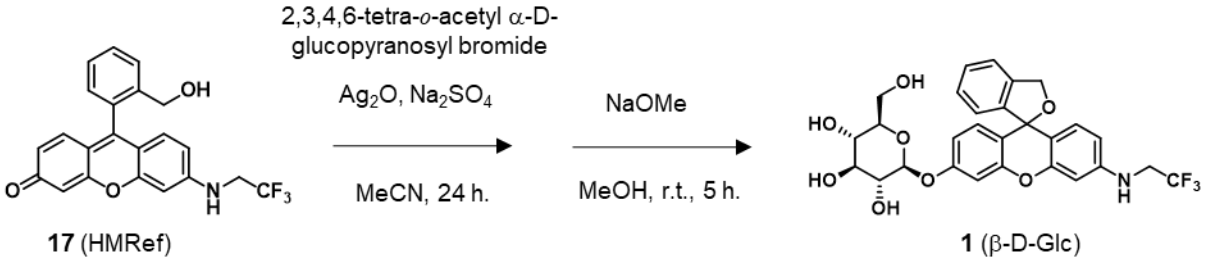

Procedure for the synthesis of 1 (β-D-Glc). A mixture of HMRef (0.426 g, 1.07 mmol), 2,3,4,6-tetra-*O*-acetyl α-D-glucopyranosyl bromide (8.26 g, 20.1 mmol), Ag_2O (4.71 g, 20.3 mmol) and Na_2SO_4 (720 mg, 2.00 mmol) in 30.0 mL dried MeCN was stirred at room temperature for 24 h. The reaction mixture was filtrated through a Celite pad, and the filtrate was concentrated under reduced pressure. The residue was purified by flash column chromatography (CH_2Cl_2 : MeOH = 95 : 5) to obtain the crude 2,3,4,6-tetra-*O*-acetyl β-D-glucopyranosylated derivative, which was dissolved in 5.00 mL dried MeOH. To this solution, NaOMe (520 mg, 9.63 mmol) dissolved in 5.00 mL dried MeOH was added dropwise, and the reaction mixture was stirred at room temperature for 5 h. The solution was neutralized with Amberlite IR 120, filtered, and concentrated under reduced pressure. The residue was purified by flash column chromatography (CH_2Cl_2 : MeOH = 9 : 1) to afford **1 (β-D-Glc)** (301 mg, 0.535 mmol) as a yellow powder in 50.2 % yield. The identity of the product was confirmed by means of ^{1}H NMR and ESI-HRMS. ^{1}H NMR (400 MHz, CD_3OD + NaOD): δ 7.38-7.45 (m, 2H), 7.28-7.31 (m, 1H), 6.96 (d, *J* = 2.4 Hz, 1H), 6.76-6.87 (m, 3H), 6.71-6.73 (m, 1H), 6.53 (d, *J* = 2.4 Hz, 1H), 6.47 (dd, *J* = 2.4 Hz, 8.4 Hz, 1H), 5.27 (s, 2H), 4.97 (d, *J* = 5.2 Hz, 1H), 3.73-3.94 (m, 4H), 3.20-3.50 (m, overlaps with HOD). ESI-HRMS (ESI +) m/z calcd. for $[M+H]^+$, 562.16833; found, 562.16944.

Scheme 3. Synthesis of probe **2** (β-D-Gal)

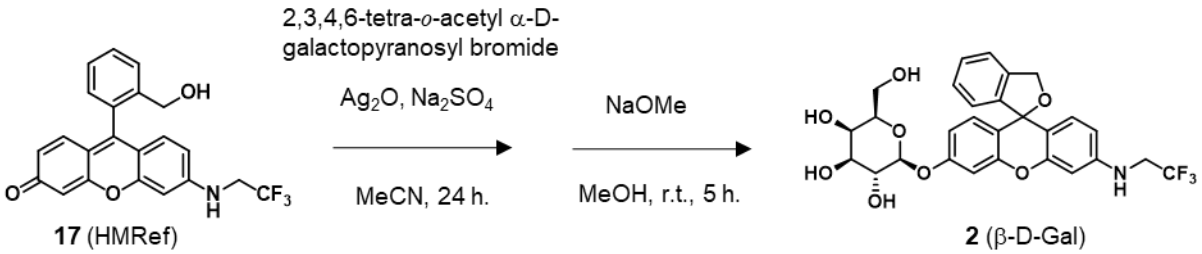

Procedure for the synthesis of 2 (β-D-Gal).[4] A mixture of HMRef (329 mg, 0.826 mmol), 2,3,4,6-tetra-*O*-acetyl α-D-galactopyranosyl bromide (6.76 g, 16.5 mmol), Ag_2O (3.83 g, 16.5 mmol) and Na_2SO_4 (500 mg, 3.34 mmol) in 40.0 mL dried MeCN was stirred at room temperature for 24 h. The reaction mixture was filtered through a Celite pad, and the filtrate was concentrated under reduced pressure to obtain the crude 2,3,4,6-tetra-*o*-acetyl β-D-galactopyranosylated derivative, which was dissolved in 10.0 mL dried MeOH. To this solution, NaOMe (2.30 g, 42.6 mmol) dissolved in 20.0 mL dried MeOH was added dropwise. The reaction mixture was stirred at room temperature for 5 h, then neutralized with Amberlite IR 120, filtered, and concentrated under reduced pressure. The residue was purified by flash column chromatography (CH_2Cl_2 : MeOH = 9 : 1) to afford **2 (β-D-Gal)** (69.1 mg, 0.123 mmol) as a yellow powder in 14.9 % yield. The identity of the product was confirmed by means of ESI-HRMS. ESI-HRMS (ESI +) m/z calcd. for $[M+H]^+$, 562.16833; found, 562.17008.

Scheme 4. Synthesis of probe **3** (β-L-Gal)

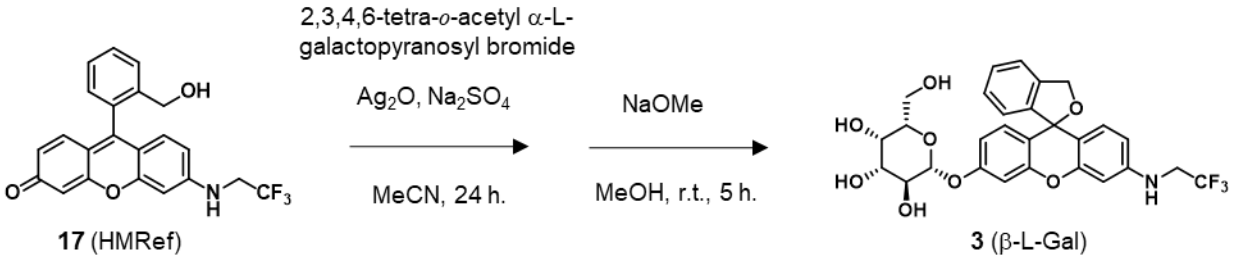

Procedure for the synthesis of 3 (β-L-Gal). 2,3,4,6-Tetra-*O*-acetyl α-L-galactopyranosyl bromide was synthesized according to the reported procedure.[5] A mixture of HMRef (92 mg, 0.230 mmol), 2,3,4,6-tetra-*O*-acetyl α-L-galactopyranosyl bromide (692 mg, 1.68 mmol), Ag_2O (430 mg, 1.85 mmol) and Na_2SO_4 (300 mg, 2.00 mmol) in 10.0 mL dried MeCN was stirred at room temperature for 24 h. The reaction mixture was filtered through a Celite pad, and the filtrate was concentrated under reduced pressure. The residue was dissolved in 15.0 mL dried MeOH. To this solution, NaOMe (900 mg, 16.7 mmol) dissolved in 5.00 mL dried MeOH was added dropwise, and the reaction mixture was stirred at room temperature for 5 h. The solution was neutralized with Amberlite IR 120, filtered, and concentrated under reduced pressure. The residue was purified by flash column chromatography (CH_2Cl_2 : MeOH = 9 : 1) to afford **3 (β-L-Gal)** (52.7 mg, 0.0937 mmol) as a yellow powder in

40.1 % yield. The identity of the product was confirmed by means of ^{1}H NMR and ESI-HRMS. ^{1}H NMR (400 MHz, CD_3OD): δ 7.40-7.27 (m, 2H), 7.13-7.16 (m, 1H), 6.84 (d, *J* = 2.4 Hz, 1H), 6.69-6.73 (m, 3H), 6.59 (d, *J* = 8.4 Hz, 1H), 6.40 (m, 1H), 6.34 (dd, *J* = 2.4 Hz, 8.8 Hz, 1H), 5.14 (s, 2H), 4.80 (d, *J* = 7.6 Hz, 1H), 4.23-4.19 (m, 1H), 3.84-3.80 (m, 2H), 3.74-3.55 (m, 7H), 3.52-3.40 (m, overlaps with HOD). ESI-HRMS (ESI +) m/z calcd. for $[M+Na]^+$, 584.15027; found, 584.15074.

Scheme 5. Synthesis of probe **4** (β-D-Xyl)

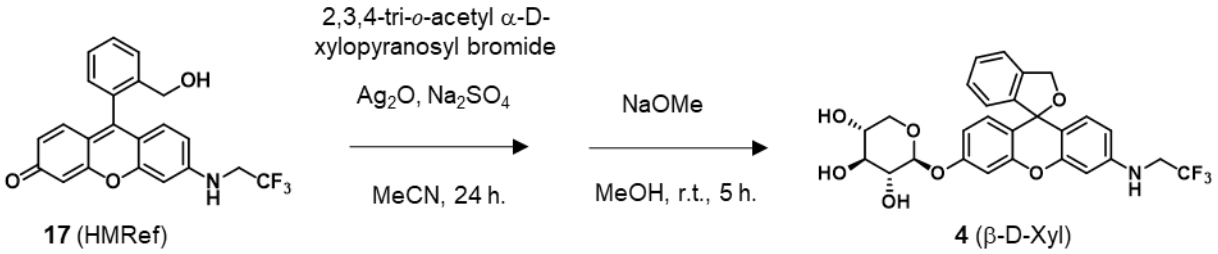

Procedure for the synthesis of 4 (β-D-Xyl). 2,3,4-Tri-*O*-acetyl α-D-xylopyranosyl bromide was synthesized according to the a literature reported procedure.[6] A mixture of **17** (107 mg, 0.268 mmol), 2,3,4-tri-*O*-acetyl α-D-xylopyranosyl bromide (3.10 g, 9.17 mmol), Ag_2O (2.10 g, 9.05 mmol) and Na_2SO_4 (500 mg, 3.34 mmol) in 25.0 mL dried MeCN was stirred at room temperature for 24 h. The reaction mixture was filtered through a Celite pad, and the filtrate was concentrated under reduced pressure. The residue was purified by flash column chromatography (CH_2Cl_2 : MeOH = 95 : 5) to afford the crude 2,3,4-tri-*O*-acetyl β-D-xylopyranosylated derivative, which was dissolved in 40.0 mL dried MeOH. To this solution, NaOMe (1.03 g, 19.1 mmol) dissolved in 5.00 mL dried MeOH was added dropwise, and the reaction mixture was stirred at room temperature for 5 h. The solution was neutralized with Amberlite IR 120, filtered, and concentrated under reduced pressure. The residue was purified by flash column chromatography (CH_2Cl_2 : MeOH = 9 : 1) to afford **4 (β-D-Xyl)** (14.8 mg, 0.0279 mmol) as a yellow powder in 10.4 % yield. The identity of the product was confirmed by means of ^{1}H NMR and ESI-HRMS. ^{1}H NMR (400 MHz, CD_3OD): δ 7.40-7.43 (m, 2H), 7.29-7.31 (m, 1H), 6.92 (d, *J* = 2.4 Hz, 1H), 6.78-6.85 (m, 3H), 6.71-6.73 (d, *J* = 8.4 Hz 1H), 6.54 (d, *J* = 2.4 Hz, 1H), 6.47 (dd, *J* = 2.4 Hz, 8.4 Hz, 1H), 5.27 (s, 2H), 4.91 (d, *J* = 7.6 Hz, 1H), 3.53-3.89 (m, 6H), 3.30-3.50 (m, overlaps with CD_3OD), 1.33 (dd, *J* = 5.2 Hz, 6.8 Hz, 3H). ESI-HRMS (ESI +) m/z calcd. for $[M+H]^+$, 532.15776; found, 532.15765.

Scheme 6. Synthesis of probe **5** (α-D-Man) (HMRef-αMan)

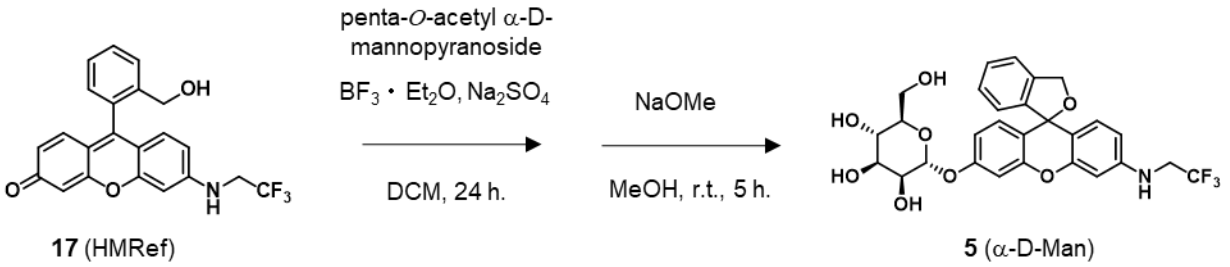

Procedure for the synthesis of 5 (α-D-Man). A mixture of HMRef (96.0 mg, 0.24 mmol), penta-*O*-acetyl-D-mannopyranoside (3.33 g, 8.53 mmol), boron trifluoride diethyl ether complex (8.0 mL, 63.4 mmol) and Na_2SO_4 (500 mg, 3.52 mmol) in 15 mL dried DCM was stirred at room temperature for 24 h. The reaction mixture was filtered through a Celite pad, and the filtrate was washed with 1 M NaOH and brine, dried over Na_2SO_4 and concentrated under reduced pressure. The residue was dissolved in 15.0 mL dried MeOH. To this solution, NaOMe (1.60 g, 29.6 mmol) dissolved in 5.0 mL dried MeOH was added dropwise, and the reaction mixture was stirred at room temperature for 5 h. The solution was neutralized with Amberlite IR 120, filtered, and concentrated under reduced pressure. The residue was purified by flash column chromatography (CH_2Cl_2 : MeOH = 9 : 1) and HPLC to afford **5 (α-D-Man)** (61.6 mg, 0.200 mmol) as a yellow powder in 45.6 % yield. The identity of the product was confirmed by means of ^{1}H NMR and ESI-HRMS. ^{1}H NMR (400 MHz, CD_3OD+NaOD): δ 7.29-7.42 (m, 2H), 7.17-7.19 (m, 1H), 6.88 (t, *J* = 2.8 Hz, 1H), 6.67-6.75 (m, 3H), 6.60 (dd, , *J* = 2.4 Hz, 8.8 Hz, 1H), 6.41 (d, *J* = 2.4 Hz, 1H), 6.36 (dd, *J* = 2.4 Hz, 8.4 Hz, 1H), 5.44 (d, *J* = 1.6 Hz, 1H), 5.14 (s, 2H), 3.91-3.93 (m, 1H), 3.63-3.82 (m, 7H), 3.46-3.51 (m, 1H), 1.19 (m, 1H). ESI-HRMS (ESI +) m/z calcd. for $[M+H]^+$, 562.16833; found, 562.17027.

Scheme 7. Synthesis of probe **6** (β-D-Fuc)

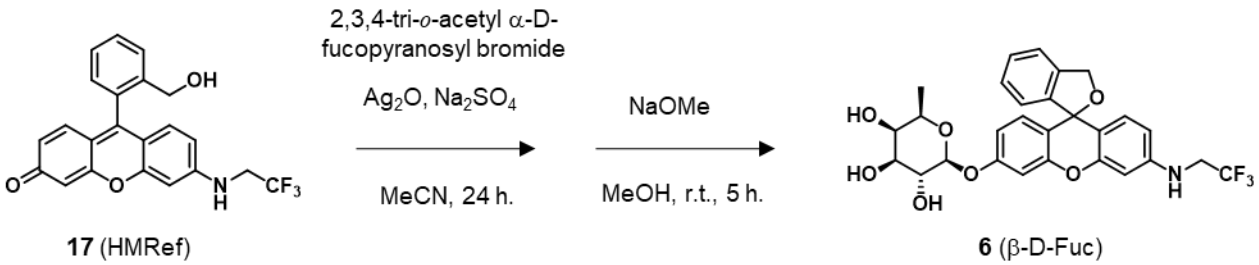

Procedure for the synthesis of 6 (β-D-Fuc). 2,3,4-Tri-*O*-acetyl α-D-fucopyranosyl bromide was synthesized according to the reported procedure.[7] A mixture of HMRef (62.0 mg, 0.155 mmol), 2,3,4-tri-*O*-acetyl α-D-fucopyranosyl bromide (2.54 g, 7.22 mmol), Ag_2O (1.72 g, 7.38 mmol) and Na_2SO_4 (400 mg, 2.67 mmol) in 25.0 mL dried MeCN was stirred at room temperature in the dark for 24 h. The mixture was filtered through a

Celite pad, and the filtrate was concentrated under reduced pressure. The residue was dissolved in 25.0 mL dried MeOH. To this solution, NaOMe (1.54 g, 28.5 mmol) dissolved in 5.00 mL dried MeOH was added dropwise, and the reaction mixture was stirred at room temperature for 5 h. The solution was neutralized with Amberlite IR 120, filtered, and concentrated under reduced pressure. The sample was dissolved in CH_2Cl_2, washed with water and brine, dried over Na_2SO_4, and concentrated. The residue was purified by flash column chromatography (CH_2Cl_2 : MeOH = 9 : 1) to afford **6 (β-D-Fuc)** (71.2 mg, 0.131 mmol) as a yellow powder in 84.2 % yield. The identity of the product was confirmed by means of ^{1}H NMR and ESI-HRMS. ^{1}H NMR (400 MHz, CD_3OD): δ 7.20-7.42 (m, 2H), 7.29-7.31 (m, 1H), 6.92 (d, *J* = 2.4 Hz, 1H), 6.82-6.85 (m, 3H), 6.71 (d, *J* = 8.4 Hz, 1H), 6.54 (d, *J* = 2.4 Hz, 1H), 6.46 (dd, *J* = 2.4 Hz, 8.4 Hz, 1H), 5.26 (s, 2H), 4.92 (d, overlaps with HOD), 3.69-3.84 (m, 4H), 3.59-3.61 (m, 1H), 3.33-3.38 (m, overlaps with CD_3OD), 1.32 (dd, *J* = 3.6 Hz, 6.4 Hz, 3H). ESI-HRMS (ESI +) m/z calcd. for $[M+Na]^+$, 568.15536; found, 568.15717.

Scheme 8. Synthesis of probe **7** (α-L-Fuc)

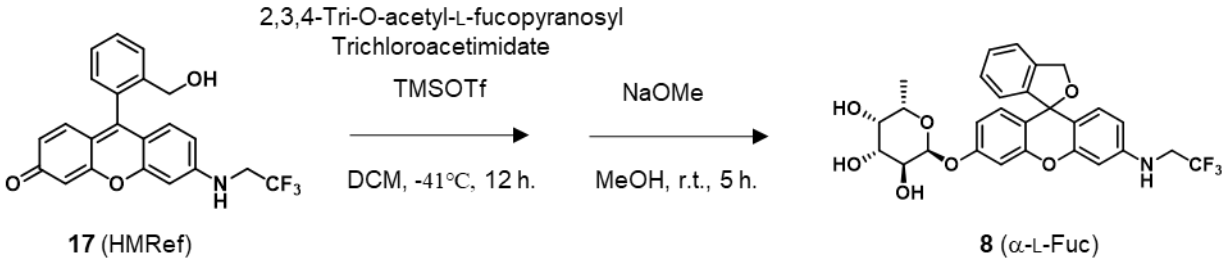

Procedure for the synthesis of 7 (α-L-Fuc). 2,3,4-Tri-O-acetyl-L-fucopyranosyl trichloroacetimidate was synthesized according to the reported procedure.[8] A mixture of **17** (90.0 mg, 0.226 mmol), 2,3,4-Tri-O-acetyl-L-fucopyranosyl trichloroacetimidate (862 mg, 1.99 mmol), and TMSOTf (442 mg, 1.99 mmol) in 10.0 mL dried CH_2Cl_2 was stirred at -41°C for 12 h. The reaction mixture was diluted with CH_2Cl_2 and neutralized with sat. $NaHCO_3$ aq. The organic layer was washed with water and brine, dried over Na_2SO_4, and concentrated under reduced pressure. The residue was purified by flash column chromatography to afford the crude 2,3,4-tri-*O*-acetyl-L-fucopyranosylated derivative, which was dissolved in 5.00 mL dried MeOH. To this solution, NaOMe (1.33 g, 24.6 mmol) dissolved in 5.00 mL dried MeOH was added dropwise, and the reaction mixture was stirred at room temperature for 5 h. The solution was neutralized with Amberlite IR 120, filtered, and concentrated under reduced pressure. The residue was purified by flash column chromatography (CH_2Cl_2 : MeOH = 95 : 5) and HPLC to afford **7 (α-L-Fuc)** (14.4 mg, 0.0257 mmol) as a yellow powder in 11.7 % yield. The identity of the product was confirmed by means of ^{1}H NMR and ESI-HRMS. ^{1}H NMR (400 MHz, CD_3OD): δ 7.29-7.32 (m, 2H), 7.18-7.19 (m, 1H), 6.87 (d, *J* = 2.0 Hz, 1H), 6.67-6.80 (m, 3H), 6.59-6.61 (d, *J* = 8.4 Hz 1H), 6.42 (d, *J* = 2.4 Hz, 1H), 6.35 (dd, *J* = 2.4 Hz, 8.4 Hz, 1H), 5.41(d, *J* = 3.2 Hz, 1H), 5.15 (s, 2H), 3.38-3.85 (m, 6H), 3.03-3.30 (m, overlaps with CD_3OD), 1.21 (dd, *J* = 5.2 Hz, 6.8 Hz, 3H), 1.09 (d, *J* = 6.4 Hz, 2H). ESI-HRMS (ESI +) m/z calcd. for $[M+H]^+$, 546.17341; found, 546.17449.

Scheme 9. Synthesis of probe **8** (β-L-Fuc)

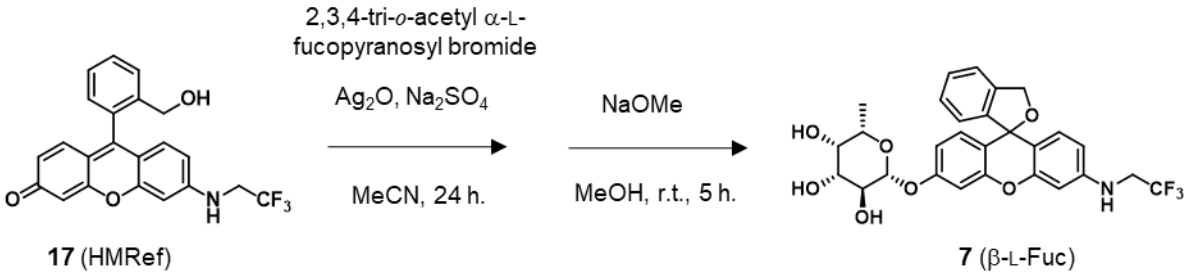

Procedure for the synthesis of 8 (β-L-Fuc). 2,3,4-Tri-*O*-acetyl α-L-fucopyranosyl bromide was synthesized according to the reported procedure.[9] A mixture of HMRef (150 mg, 0.453 mmol), 2,3,4-tri-*O*-acetyl α-L-fucopyranosyl bromide (3.20 g, 9.09 mmol), Ag_2O (2.11 g, 9.05 mmol) and Na_2SO_4 (500 mg, 3.34 mmol) in 25.0 mL dried MeCN was stirred at room temperature in the dark for 24 h. The reaction mixture was filtered through a Celite pad, and the filtrate was concentrated under reduced pressure. The residue was purified by flash column chromatography (CH_2Cl_2 : MeOH = 95 : 5) to afford the crude 2,3,4-tri-*O*-acetyl β-L-fucopyranosylated derivative, which was dissolved in 15.0 mL dried MeOH. To this solution, NaOMe (320 mg, 5.93 mmol) dissolved in 5.00 mL dried MeOH was added dropwise, and the reaction mixture was stirred at room temperature for 5 h. The solution was neutralized with Amberlite IR 120, filtered, and concentrated under reduced pressure. The residue was purified by flash column chromatography (CH_2Cl_2 : MeOH = 9 : 1) to afford **8 (β-L-Fuc)** (140 mg, 0.257 mmol) as a yellow powder in 56.8 % yield. The identity of the product was confirmed by means of ^{1}H NMR and ESI-HRMS. ^{1}H NMR (400 MHz, CD_3OD): δ 7.40-7.43 (m, 2H), 7.29-7.31 (m, 1H), 6.92 (d, *J* = 2.4 Hz, 1H), 6.78-6.85 (m, 3H), 6.72 (d, *J* = 8.4 Hz 1H), 6.54 (d, *J* = 2.4 Hz, 1H), 6.47 (dd, *J* = 2.4 Hz, 8.4 Hz, 1H), 5.27 (s, 2H), 4.91 (d, *J* = 7.6 Hz, 1H), 3.53-3.89 (m, 6H), 3.30-3.50 (m, overlaps with CD_3OD), 1.33 (dd, *J* = 3.6 Hz, 6.8 Hz, 3H). ESI-HRMS (ESI +) m/z calcd. for $[M+Na]^+$, 568.15536; found, 568.15638.

Scheme 10. Synthesis of probe **9** (α-D-Ara)

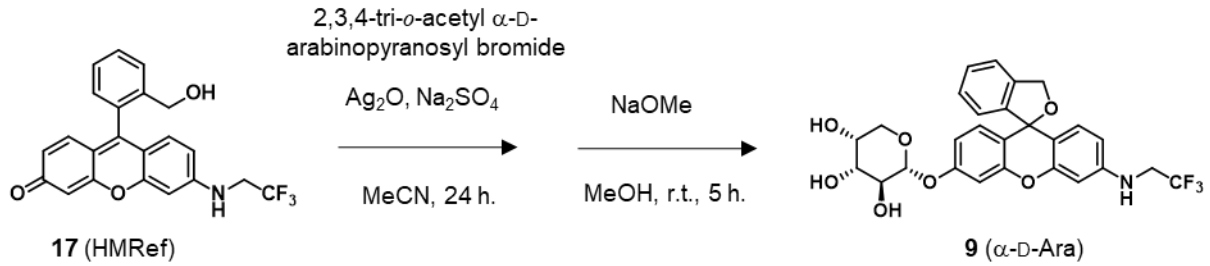

Procedure for the synthesis of 9 (α-D-Ara). 2,3,4-Tri-O-acetyl-β-D-arabinopyranosyl bromide was synthesized according to the reported procedure.[10] A mixture of HMRef (85.3 mg, 0.214 mmol), crude 2,3,4-tri-*O*-acetyl β-D-arabinopyranosyl bromide (2.94 g), Ag_2O (1.70 g, 7.33 mmol) and Na_2SO_4 (700 mg, 4.93 mmol) in 10.0 mL dried MeCN was stirred at room temperature for 24 h. The reaction mixture was filtered through a Celite pad, and the filtrate was concentrated under reduced pressure. The residue was dissolved in 15.0 mL dried MeOH. To this solution, NaOMe (800 mg, 14.8 mmol) dissolved in 5.00 mL dried MeOH was added dropwise, and the reaction mixture was stirred at room temperature for 5 h. The solution was neutralized with Amberlite IR 120, filtered, and concentrated under reduced pressure. The residue was purified by flash column chromatography (CH_2Cl_2 : MeOH = 9 : 1) to afford **9 (α-D-Ara)** (52.8 mg, 0.0994 mmol) as a yellow powder in 46.4 % yield. The identity of the product was confirmed by means of ^{1}H NMR and ESI-HRMS. ^{1}H NMR (400 MHz, CD_3OD + K_2CO_3): δ 7.27-7.32 (m, 2H), 7.16-7.18 (m, 1H), 6.80 (d, *J* = 2.4 Hz, 1H), 6.70-6.74 (m, 3H), 6.66 (m, 1H), 6.59 (d, *J* = 9.2 Hz, 1H), 6.41 (d, *J* = 2.0 Hz, 1H), 6.34 (dd, *J* = 2.4 Hz, 8.8 Hz, 1H), 5.14 (s, 2H), 4.79 (d, overlaps with HOD), 3.69-3.85 (m, 5H), 3.60-3.64 (m, 1H), 3.55 (dd, *J* = 3.6 Hz, 9.2 Hz, 1H). ESI-HRMS (ESI +) m/z calcd. for $[M+Na]^+$, 554.13971; found, 554.14023.

Scheme 11. Synthesis of probe **10** (α-L-Ara)

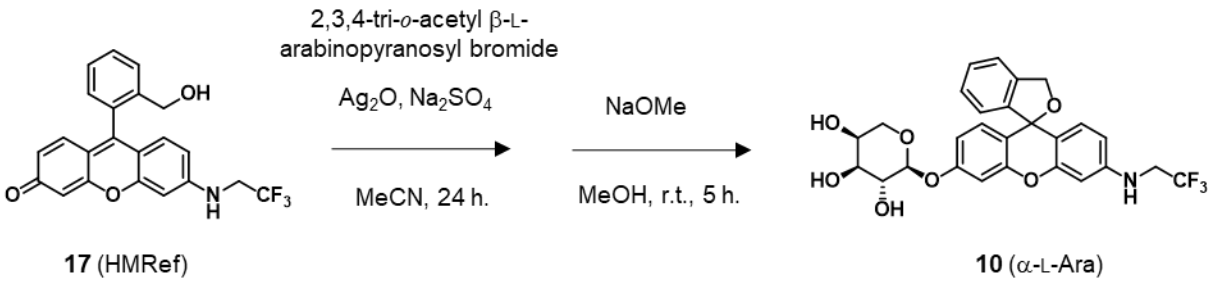

Procedure for the synthesis of 10 (α-L-Ara). 2,3,4-Tri-O-acetyl-β-L-arabinopyranosyl bromide was synthesized according to the reported procedure.[10] A mixture of HMRef (84.0 mg, 0.211 mmol), 2,3,4-tri-*O*-acetyl-β-L-arabinopyranosyl bromide (1.09 mg), Ag_2O (747 mg, 3.21 mmol) and Na_2SO_4 (520 mg, 3.66 mmol) in 10.0 mL dried MeCN was stirred at room temperature for 24 h. The reaction mixture was filtered through a Celite pad, and the filtrate was concentrated under reduced pressure. The residue was dissolved in 15.0 mL dried MeOH. To this solution, NaOMe (500 mg, 9.26 mmol) dissolved in 5.00 mL dried MeOH was added dropwise, and the reaction mixture was stirred at room temperature for 5 h. The solution was neutralized with Amberlite IR 120, filtered, and concentrated under reduced pressure. The residue was purified by flash column chromatography (CH_2Cl_2 : MeOH = 9 : 1) to afford **10 (α-L-Ara)** (27.1 mg, 0.0994 mmol) as a yellow powder in 24.2 % yield. ^{1}H NMR (400 MHz, CD_3OD + K_2CO_3): δ 7.39-7.43 (m, 2H), 7.26-7.32 (m, 1H), 6.92 (d, *J* = 2.4 Hz, 1H), 6.83-6.86 (m, 2H), 6.75-6.80 (m, 1H), 6.71 (d, *J* = 8.8 Hz, 1H), 6.53 (d, *J* = 2.4 Hz, 1H), 6.47 (dd, *J* = 2.4 Hz, 8.8 Hz, 1H), 5.26 (s, 2H), 4.91 (d, *J* = 7.2 Hz, 1H), 3.93-3.98 (m, 1H), 3.81-3.91 (m, 4H), 3.72-3.76 (m, 1H), 3.66 (dd, *J* = 3.2 Hz, 8.8 Hz, 1H). ESI-HRMS (ESI +) m/z calcd. for $[M+Na]^+$, 554.13971; found, 554.14035.

Scheme 12. Synthesis of probe **11** (β-D-GlcNAc)

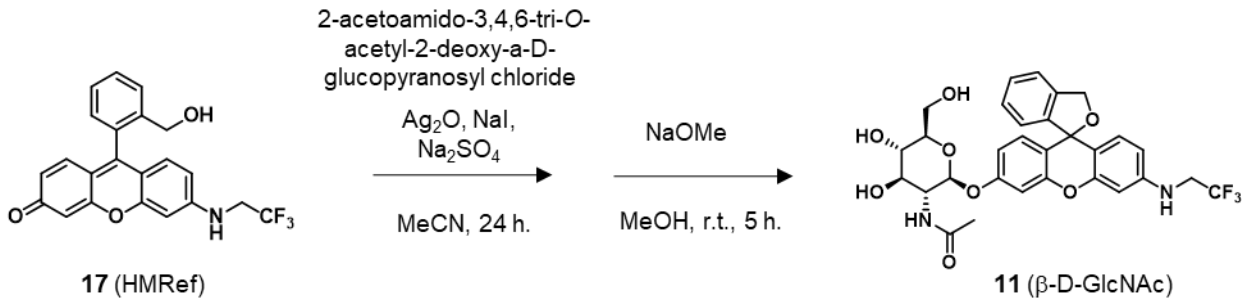

Procedure for the synthesis of 11 (β-D-GlcNAc). Compound **11 (β-D-GlcNAc)** was synthesized according to the reported procedure.[11]

Scheme 13. Synthesis of probe **12** (β-D-GalNAc)

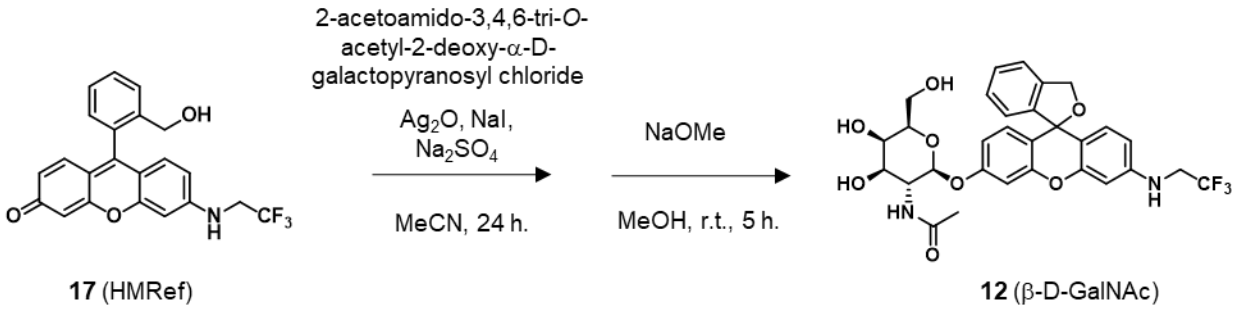

Procedure for the synthesis of 12 (β-D-GalNAc). 2-Acetoamide-3,4,6-tri-*O*-acetyl-2-deoxy-α-D-galactopyranosyl chloride was synthesized according to the reported procedure.[12] A mixture of HMRef (46.7 mg, 0.117 mmol), 2-acetoamide-3,4,6-tri-*O*-acetyl-2-deoxy-α-D-galactopyranosyl chloride (400 mg, 1.09 mmol), Ag_2O (400 mg, 1.72 mmol), NaI (88.3 mg, 0.589 mmol) and Na_2SO_4 (500 mg, 3.34 mmol) in 10 mL dried MeCN was stirred at room temperature for 24 h. The reaction mixture was filtered through a Celite pad, and the filtrate was concentrated under reduced pressure to give the crude 2-acetoamide-3,4,6-tri-*O*-acetyl-2-deoxy-β-D-galactopyranosylated derivative, which was dissolved in 10 mL dried MeOH. To this solution, NaOMe (500 mg, 9.25 mmol) dissolved in 5 mL dried MeOH was added dropwise, and the reaction mixture was stirred at room temperature for 5 h. The solution was neutralized with Amberlite IR 120, filtered, and concentrated under reduced pressure. The residue was subjected into flash column chromatography (CH_2Cl_2 : MeOH = 8 : 2) to remove unreacted sugars and salts. The crude product was purified by HPLC to afford **12 (β-D-GalNAc)** (11.3 mg, 0.0216 mmol) as a yellow powder in 28.2 % yield. The identity of the product was confirmed by means of ^{1}H NMR and ESI-HRMS. ^{1}H NMR (400 MHz, CD_3OD + K_2CO_3): δ 7.28-7.33 (m, 2H), 7.17-7.19 (m, 1H), 6.78 (d, *J* = 2.4 Hz, 1H), 6.68-6.74 (m, 2H), 6.59-6.63 (m, 2H), 6.40 (d, *J* = 2.4 Hz, 1H), 6.35 (dd, *J* = 2.4 Hz, 8.4 Hz, 1H), 5.14 (s, 2H), 4.95 (d, *J* = 8.4 Hz, 1H), 4.07-4.12 (m, 1H),), 3.83 (d, *J* = 3.2 Hz, 1H), 3.56-3.77 (m, 6H), 3.25 (s, 4H), 1.88 (d, *J* = 2.8 Hz, 3H). ESI-HRMS (ESI +) m/z calcd. for $[M+Na]^+$, 625.17682; found, 625.17727.

Scheme 14. Synthesis of gGlu-2OMe-SiR600.

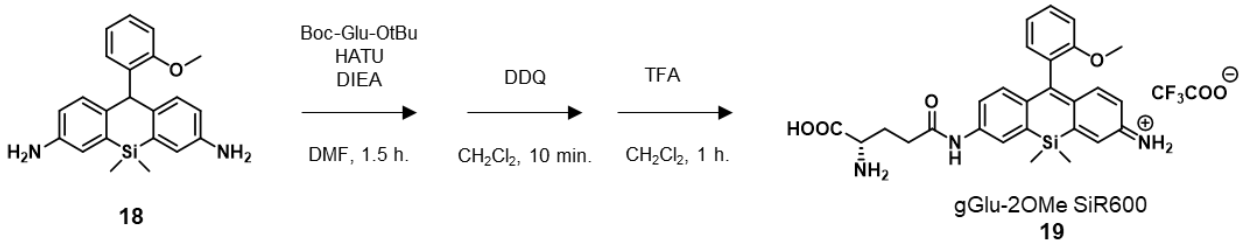

Procedure for the synthesis of 19 (gGlu-2OMe SiR600). Compound **18** was synthesized according to the reported procedure.[13] A solution of **18** (60.0 mg, 0,167 mmol), Boc-Glu-OtBu (26.0 mg, 0.0857 mmol), HATU (31.0 mg, 0.0816 mmol) and diisopropylethylamine (DIEA) (71 μL, 0.417 mmol) in 6 mL DMF was stirred at r.t. for 1.5 h, and then concentrated under reduced pressure. The residue was dissolved in CH_2Cl_2. The organic layer was washed with H_2O and brine, dried over Na_2SO_4, and concentrated. The residue was dissolved in 8 mL CH_2Cl_2. To this solution was added 2,3-dichloro-5,6-dicyano-p-benzoquione (DDQ) (76.0 mg, 0.335 mmol). The mixture was stirred at room temperature for 10 min, and then evaporated. The residue was dissolved in 3 mL CH_2Cl_2, and to this solution was added 3 mL TFA. The mixture was stirred at r.t. for 1 h, and then concentrated under reduced pressure. The crude product was purified by HPLC under the following conditions to afford **19**, gGlu-2OMe SiR600, (22.9 mg, 0.0469 mmol) in 45.9 % yield. Gradient elution, A/B = 70/30 to 0/100 in 40 min (eluent A: H_2O containing 0.1 % TFA, eluent B: 0.1 % TFA in 80 % acetonitrile and 20 % H_2O). The identity of the product was confirmed by means of ^{1}H NMR and ESI-HRMS. ^{1}H NMR (300 MHz, CD_3OD, isomer mixture): δ 8.22 (dd, *J* = 1.8 Hz, 7.7 Hz, 0.2H), 8.12 (d, *J* = 2.2 Hz, 0.85H), 7.82 (d, *J* = 2.2 Hz, 0.15H), 7.58-7.64 (m, 1.8H), 7.44-7.45 (m, 0.2H), 7.38-7.40 (m, 1.8H), 7.24 (d, *J* = 8.8 Hz, 1H), 7.11-7.15 (m, 3H), 6.76 (dd, *J* = 2.2 Hz, 9.5 Hz, 0.8H), 6.68 (d, *J* = 8.1 Hz, 0.2H), 4.02 (t, *J* = 6.6 Hz, 1H), 3.72 (s, 2.4H), 3.07 (s, 0.6H), 2.66-2.77 (m, 2H), 2.19-2.33 (m, 2H), 0.59 (s, 3H), 0.56 (s, 2.4H), 0.45 (s, 0.6H). ESI-HRMS (ESI +) m/z calcd. for $[M+H]^+$, 488.20056; found, 488.19990.

References

1. Urano, Y., *et al.* Rapid Cancer Detection by Topically Spraying a γ-Glutamyltranspeptidase–Activated Fluorescent Probe. *Science Translational Medicine* **3**, 110ra119-110ra119 (2011).

2. Komatsu, T., *et al.* Diced Electrophoresis Gel Assay for Screening Enzymes with Specified Activities. *Journal of the American Chemical Society* **135**, 6002-6005 (2013).

3. He, L., *et al.* α-Mannosidase 2C1 attenuates PTEN function in prostate cancer cells. *Nature Communications* **2**, 307 (2011).

4. Asanuma, D., *et al.* Sensitive β-galactosidase-targeting fluorescence probe for visualizing small peritoneal metastatic tumours in vivo. *Nature Communications* **6**, 6463 (2015).

5. Wolf, S., Berrio, R.M. & Meier, C. Synthesis of Nonnatural Nucleoside Diphosphate Sugars. *European Journal of Organic Chemistry* **2011**, 6304-6313 (2011).

6. Mitchell, S.A., Pratt, M.R., Hruby, V.J. & Polt, R. Solid-Phase Synthesis of O-Linked Glycopeptide Analogues of Enkephalin. *The Journal of Organic Chemistry* **66**, 2327-2342 (2001).

7. Faust, T., Theurer, C., Eger, K. & Kreis, W. Synthesis of Uridine 5′-(β-D-Fucopyranosyl Diphosphate) and (Digitoxigenin-3β-yl)-β-D-Fucopyranoside and Enzymatic β-D-Fucosylation of Cardenolide Aglycones in Digitalis lanata1. *Bioorganic Chemistry* **22**, 140-149 (1994).

8. Schmidt, R.R., Wegmann, B. & Jung, K.-H. Glycosyl imidates, 47. Stereospecific synthesis of α- and □-L-fucopyranosyl phosphates and of gdp-fucose via trichloroacetimidate. *Liebigs Annalen der Chemie* **1991**, 121-124 (1991).

9. Boutureira, O., Bernardes, G.J.L., Fernández-González, M., Anthony, D.C. & Davis, B.G. Selenenylsulfide-Linked Homogeneous Glycopeptides and Glycoproteins: Synthesis of Human "Hepatic Se Metabolite A". *Angewandte Chemie International Edition* **51**, 1432-1436 (2012).

10. Doyle, L.M., *et al.* Stereoselective Epimerizations of Glycosyl Thiols. *Organic Letters* **19**, 5802-5805 (2017).

11. Matsuzaki, H., *et al.* Novel Hexosaminidase-Targeting Fluorescence Probe for Visualizing Human Colorectal Cancer. *Bioconjugate Chemistry* **27**, 973-981 (2016).

12. Boutureira, O., Bernardes, G.J.L., Fernández-González, M., Anthony, D.C. & Davis, B.G. Selenenylsulfide-Linked Homogeneous Glycopeptides and Glycoproteins: Synthesis of Human "Hepatic Se Metabolite A". *Angewandte Chemie International Edition* **51**, 1432-1436 (2012).

13. Ogasawara, A., *et al.* Red Fluorescence Probe Targeted to Dipeptidylpeptidase-IV for Highly Sensitive Detection of Esophageal Cancer. *Bioconjugate Chemistry* **30**, 1055-1060 (2019).